Check for updates

Adapting to rapidly transforming seascapes in the Mid- to Late Holocene, southeastern Australia

Ashleigh J. Rogers [1,2]*, David M. Kennedy [1,3], Bruno David [1,2], Russell Mullett[1,4], Joanna Fresløv[4], Fiona Petchey [5,6], Lee J. Arnold [7], Martina Demuro [7], GunaiKurnai Land and Waters Aboriginal Corporation[1,4], Cheryl Drayton[4] and Howard Mullett[4]

[1]ARC Centre of Excellence for Australian Biodiversity and Heritage, Monash University, Clayton, VIC, Australia, [2]Monash Indigenous Studies Centre, Monash University, Clayton, VIC, Australia, [3]School of Geography, Earth and Atmospheric Sciences, The University of Melbourne, Parkville, VIC, Australia, [4]GunaiKurnai Land and Waters Aboriginal Corporation, Bairnsdale, VIC, Australia, [5]Radiocarbon Dating Laboratory, University of Waikato, Hamilton, New Zealand, [6]ARC Centre of Excellence for Australian Biodiversity and Heritage, James Cook University, Cairns, QLD, Australia, [7]School of Physics, Chemistry and Earth Sciences, Environment Institute and Institute for Photonics and Advanced Sensing, University of Adelaide, Adelaide, SA, Australia

Aquatic environments are highly dynamic. They are characterized by rapid and often unpredictable transformations driven by sea-level fluctuations, climate change, tectonic activity, and anthropic land-and-sea use practices that result in large-scale environmental shifts. Globally, archaeology has documented how people adapt and respond to these changes by altering subsistence strategies, settlement patterns, travel routes, and technologies to meet the challenges of a constantly transforming aquascape. Coastal regions, in particular, have both challenged and sustained human populations, offering abundant resources while also requiring significant adaptability in response to regular and, at times, substantial sea level fluctuations from the terminal Pleistocene throughout the Holocene. Using an interdisciplinary approach that pairs coastal geomorphology and archaeology, we investigated the Mid- to Late Holocene development of a barrier island in southeast Victoria, Australia—the development of which prompted wider inshore ecosystem transformations. Results from archaeological excavations demonstrate that people responded to coastal transformations by flexibly adjusting their lifeways and subsistence strategies over short time-scales and, through firing of the landscape, shaped surrounding ecosystems in return. Understanding how populations navigated these past changes, both through immediate adaptive responses and long-term cultural transformations, provides valuable insights into the resilience and adaptability of human societies in the face of environmental uncertainty.

KEYWORDS

coastal geomorphology, barrier island development, island and coastal archaeology, shell midden studies, coastal transformation, Holocene, cultural burning, southeast Australia

1 Introduction

Aquascapes, with their rich ecosystems and diverse resources, have been important environments through the course of human history. They have played major roles in the early peopling of continents and islands (Erlandson et al., 2015; Erlandson and Braje, 2015) and been focal places of subsistence and food production (Will et al., 2022;

Rogers, 2023), trade and exchange (Collerson and Weisler, 2007; Fitzpatrick and Anderson, 2008), travel and exploration (Fitzpatrick, 2009; Skelly and David, 2017), and technological innovation (Johns et al., 2014; Pedergnana et al., 2021). Aquatic environments are also highly dynamic, characterized by rapid and often unpredictable transformations driven by sea-level fluctuations, climate change and tectonic activity that result in large-scale environmental shifts (Krapivner, 2020). Aquatic systems also connect land masses with the sea at critical junctures; it is through waterways that loosened sediments from gardening are carried to river deltas and along coastlines, for example, prograding the available landmass and all that it contains (David et al., 2020; Fitzpatrick and Giovas, 2021; Rogers and Weisler, 2024; Rowe et al., 2020). Coastal regions have experienced some of the most significant environmental changes, particularly during the marine transgression of the terminal Pleistocene and subsequent Early to Mid-Holocene sea level rise, where vast tracts of land were inundated, landforms migrated inland, connecting land-bridges disappeared and where near-coastal, coastal, and littoral environments (and their attendant biota) were transformed (Hibbert et al., 2018; see also Gusick et al., 2022; Hristova and Peev, 2014; Surdez et al., 2018).

Globally, archaeology has documented how people adapted to dynamic coastal environmental conditions. Frequently, human responses have included shifting subsistence strategies in light of habitat changes, with communities often focusing on those elements of the ecosystem considered stable and rich in reliable food resources, such as molluscs (Codding et al., 2014; Faulkner et al., 2022; Rogers and Weisler, 2022). At Bubog I and II in the Philippines, for example, Pawlik et al. (2014) documented that during the Late Pleistocene people harvested intertidal mangrove invertebrates (e.g., molluscs: *Terebralia* spp., *Telescopium* spp., *Geloina coaxans*; crabs: *Scylla* spp.) at a time of low sea levels and expansive mangrove habitats. In the Early Holocene, sea levels rose and inundated the mangroves, creating a brackish shallow marine environment. This habitat change meant people then harvested brackish and shallow marine molluscs (e.g., *Nerita undata*, *Angaria delphinus*). By the Mid-Holocene, as sea levels continued to rise, they then gathered exclusively marine invertebrates that indicated the presence of a lagoon and coral reef (e.g., numerous *Tridacna* and *Hippopus* taxa; Pawlik et al., 2014, pp. 237–239). Similar subsistence trends were identified by Marwick et al. (2017) at Khao Toh Chong rockshelter, Thailand, where diets shifted away from freshwater resources (gastropods, turtles) to mangrove-dwelling species as intertidal environments moved closer to the rockshelter as sea levels rose.

Archaeology has also documented the development or expansion of food-producing technologies in response to changing environments. On the Isles of Scilly, northwest Europe, Barnett et al. (2020) found that, instead of leaving the forested Scilly landmass as it gradually fragmented into a series of grass-covered islands, people instead introduced grazing stock, established additional settlements, and constructed monumental architecture (e.g., cairns, standing stones, entrance graves). Food production as an adaptive strategy was not limited to the terrestrial landscape. Increasingly, archaeologists have documented people responding to aquatic transformations by proactively shaping aquascapes to meet the demands and socio-environmental opportunities of the time (see review and discussion in Salomon and McKechnie, 2025 and Rogers, 2023). Such dynamic interactions between people and their local aquascapes are particularly evident archaeologically in regions where the coastal geomorphology and local hydrology have been modified by the creation of enduring structures, such as fishponds, traps and weirs, and shellfish gardens (McCoy et al., 2016; Moss, 2013; Rowland and Ulm, 2011; Smith et al., 2019). The appearance of such engagements is frequently linked to large-scale climatic changes and their resulting environmental shifts. For example, the development of walled fishponds at the site of Mound Key in Florida, USA and the appearance of clam gardens in Micronesia have been correlated with increased precipitation of the Medieval Warm Period across the Pacific (Cobb et al., 2003; Field and Lape, 2010; Thompson et al., 2014, 2018). The appearance of rice paddy agriculture and carp aquaculture has been associated with sea-level high-stands of the Early Holocene "climatic optimum" in China (Nakajima et al., 2019; Chen et al., 2005; Zhuang and Kidder, 2014), and the construction of monumental fishponds in the Hawaiian Islands has been linked to climate instability associated with increased El Niño Southern Oscillation (ENSO) frequency and following rapid cooling and sea-level fall (Nunn et al., 2007; see Rogers, 2023 for review).

Changing subsistence regimes was not the only way that people responded to fluctuating aquascapes. Other responses to aquatic transformations include large-scale population migration (Brisset et al., 2018), extension of social networks (Schmich, 2013), new travel routes and the development or acquisition of new technologies (e.g., watercraft) to access people, places or resources (Barker, 1991; Lamb and Barker, 2001), and the codification of environmental change into local cosmologies (Carson and Athens, 2007). The adaptive strategies of coastal communities in the past, in response to sea level rise and rapid coastal environmental transformations, reveal remarkable flexibility and innovation, and cultural responses are varied. These responses provide valuable insights into the long-term interactions between people and their environments, offering lessons for understanding contemporary challenges posed by climate change and sea level rise.

Here, we apply an interdisciplinary approach that pairs archaeology and coastal geomorphology to investigate the Mid- to Late Holocene development of a barrier island in southeast Victoria, Australia. Through archaeological and coastal geomorphological data, we investigate people's responses to the formation of a new near-shore island and the associated wider ecosystem transformations along the coastline.

2 Study area, environmental context, and archaeological site

The study area is a coastal barrier dune located in the eastern portion of Nooramunga Marine and Coastal Park, at the junction of McLoughlins Beach township and the Ninety-Mile Beach, coastal Gippsland, southeast Victoria, Australia (Figure 1). It marks the southern limit of the Ninety-Mile Beach Barrier sequence that represents a complex of foredune barrier ridges and back barrier estuaries and lakes with a depositional history dating back to the

Penultimate Interglacial Period (Kennedy et al., 2020, 2024). The Gippsland region of Victoria is in the Country of GunaiKurnai First Peoples (GunaiKurnai Land and Waters Aboriginal Corporation, 2015).

The coastal barrier dune is 7 km long and connected to the mainland at its northern end. Its southern end is accessible via a footbridge at the McLoughlins Beach township jetty or via boat. The eastern (open-ocean) side of the McLoughlins Beach barrier dune system is a microtidal high-energy, wave-dominated sandy beach that is open to Bass Strait. The mean significant wave height is 2.4 m with a period of 8.4 s (Hughes and Heap, 2010), with the wind and wave regime strongly linked to the annual movement of the subtropical ridge (O'Grady et al., 2015). The western side of the barrier is a low-energy estuarine sandy beach fronting a lagoon, with a large tidal flat (up to 200 m wide) at intertidal to shallow subtidal elevations, that is composed of sandy to muddy sediment with increasing distance from the shore. A channel (McLoughlins Channel) is meters deep and up to 50 m wide (main channel component) and truncates the western edge of the intertidal flat (Figures 1, 2). The estuary has extensive seagrass beds (*Zostera muelleri*, *Heterozostera tasmanica*, *Posidonia australis*, and *Halophila australis*), and supports a large population of black swans (*Cygnus atratus*). The vegetation is coastal saltbush (*Atriplex cinerea*) along the shoreline, giving way to grasses (*Lomandra* spp.), bracken fern (*Pteridium esculentum*), tea-tree (*Leptospermum* spp.), she-oak (*Casuarina*), coastal banksia (*Banksia integrifolia*), and coastal manna gum (*Eucalyptus viminalis* ssp. *pryoriana*). Toward the channel's exit into the open ocean at New Entrance, the southwest end of the barrier dune supports a saltmarsh community of beaded and shrubby glassworts (*Salicornia quinqueflora*, *Sclerostegia arbuscula*, and *Suaeda australis*) and sedges (*Lepidosperma gladiatum*), rushes (*Juncus kraussii*), and reeds (*Phragmites australis*; Figure 2). The coastal woodland is home to a variety of animals such as the swamp antechinus (*Antechinus minimus*), ground parrot (*Pezoporus wallicus*), white-bellied sea eagle (*Haliaeetus leucogaster*), eastern gray kangaroo (*Macropus giganteus*), swamp wallaby (*Wallabia bicolor*), and echidna (Tachyglossidae). The McLoughlins Beach jetty is a popular boat launch for both recreational and commercial fishers. Common catches include flathead (*Platycephalus fuscus*), garfish (*Hyporhamphus australis*), snapper (*Pagrus auratus*), King George whiting (*Sillaginodes punctatus*), Australian salmon (*Arripis trutta*), and gummy shark (*Mustelus antarcticus*). The large tidal flat on the lagoon side of the coastal barrier dune is popular today for gathering small clams, particularly sand cockles (*Katelysia* spp.).

An exposed archaeological site, Nooramunga Midden Complex, is located in the dunes on the western (estuarine) side of the coastal barrier, facing the lagoon and large tidal flat (Figures 1, 3). Eroding shell remains and the sites' associated expansive gray-brown sediment horizon is intermittently visible in the dune profile along some 800 m length of shoreline. The Nooramunga Midden Complex (Victoria Aboriginal Heritage Registry site number: VAHR 8220-0163) was registered on the Victorian state registry in 2021 and, at the time, was recommended for salvage excavation as it was considered to be in a poor and eroding condition due to visitor impacts, floods and rising sea levels. Long-term stability was considered compromised by these impacts and there was concern that the site would be gradually destroyed.

3 Methodology

3.1 Coastal barrier dune geomorphic investigations

The subsurface of the back barrier was manually sampled using a 76 mm diameter sand auger. Unconsolidated sediment samples were collected at 0.5 m intervals, as well as at depths where a change in sedimentology was observed. Two single-grain optically stimulated luminescence (OSL) dating samples were collected from above and below Nooramunga Midden Complex at the McLoughlins Beach 1 excavation (see below). Sample MLB1 was collected from the back wall of the excavation area, 30 cm below the surface of the pit, while sample MLB2 was obtained from a vertical auger hole drilled to a depth of 1.69 m below the excavation surface (equivalent to a depth of 2.8 m below the top of the excavation pit). OSL samples were taken using 200 mm-long steel tubes (63 mm diameter), which were either hammered horizontally into the face of the excavation (MLB1) or attached to a custom-designed auger head and driven vertically into the base of the auger hole (MLB2; see Supplementary file for details of OSL procedures).

Aerial surveying was undertaken using a Da-Jiang Innovations (DJI) Phantom Real-Time Kinematic (RTK) unoccupied aerial vehicle (UAV). UAV surveys were conducted at an altitude of 100 m, with vertical photography, overlapping at >70%, being processed in the software Pix4D through Structure-from-Motion principles to generate 3D point-clouds. These points were then meshed to produce a 3D digital surface model (DSM). The digital surface model has a vertical (RMS) accuracy of 0.089 m (Pucino et al., 2021) and horizontal accuracy of 0.01 m (Propeller., 2023). A single Smart-Ground Control Point (GCP) ensured positional precision, with the entire survey referenced to the Australian Height Datum where zero is equivalent to current Mean Sea Level (MSL) elevation. The full details of the methodology and processing workflows, including detailed information of the quality assurance and control of the datasets can be found in Ierodiaconou et al. (2022) and Pucino et al. (2021).

3.2 Nooramunga Midden Complex archaeological excavations

Two locations were excavated at the Nooramunga Midden Complex in March 2023, McLoughlins Beach 1 and McLoughlins Beach 2 (Figures 1, 3). McLoughlins Beach 1 was located approximately 480 m south from the footbridge in a sandy dune sequence on the western (estuarine) side of the coastal barrier. Here a 50 × 50 cm excavation square was laid, its northwest–southeast axis aligned along a compass bearing of 153° to follow the orientation of the dune edge. The square was positioned over a concentration of shell in a dark brown-gray sediment horizon, visible from the eroding dune face (Figure 3). This specific part of the midden was chosen for excavation as it appeared the least affected by undercutting erosion, tree roots, and wombat burrows compared to surrounding areas.

McLoughlins Beach 2 was located in the same dune formation, 200 m southwest of McLoughlins Beach 1 (Figure 3). Here a 25 × 25 cm excavation square was laid, its northeast–southwest axis
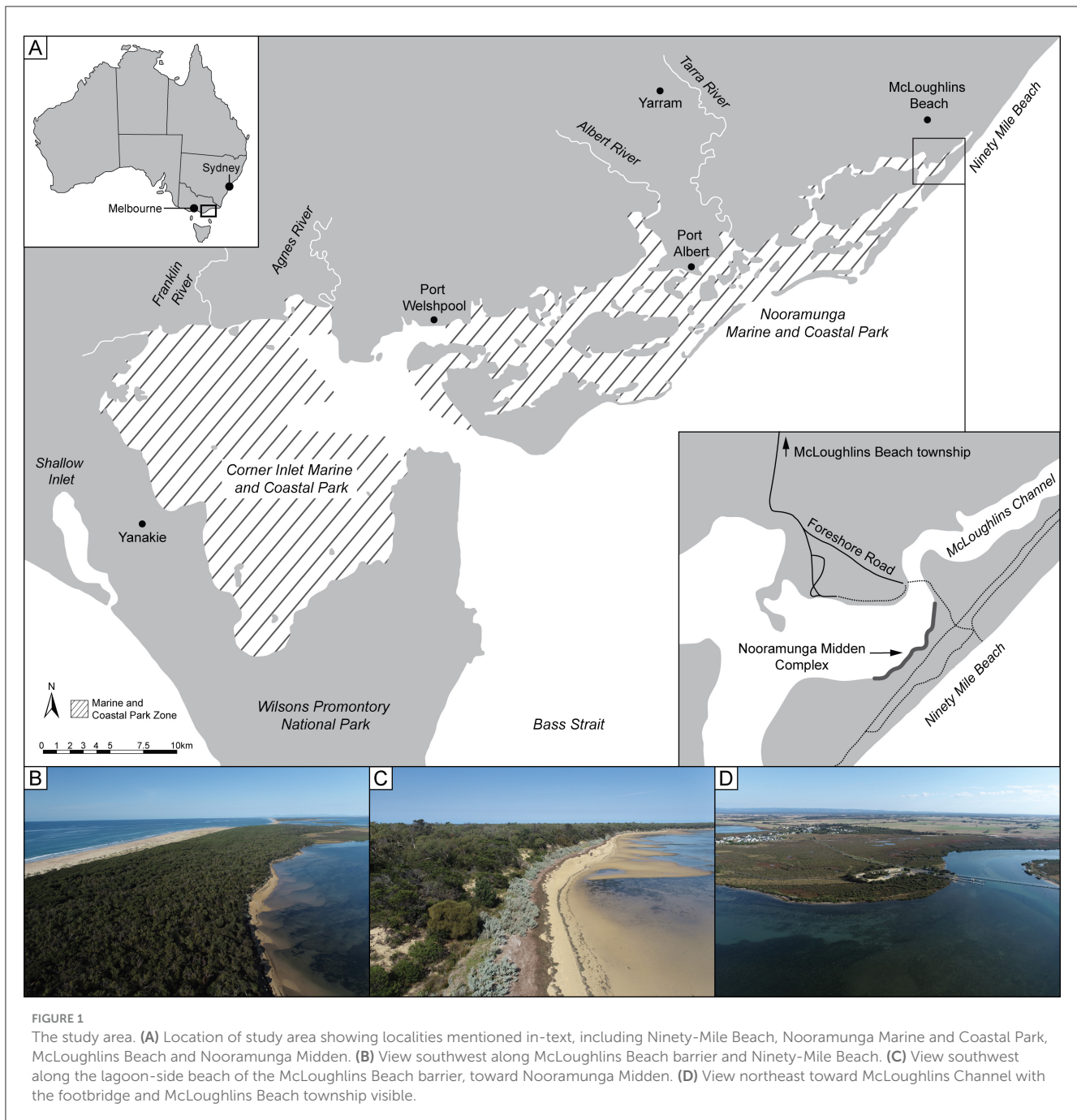
FIGURE 1
The study area. **(A)** Location of study area showing localities mentioned in-text, including Ninety-Mile Beach, Nooramunga Marine and Coastal Park, McLoughlins Beach and Nooramunga Midden. **(B)** View southwest along McLoughlins Beach barrier and Ninety-Mile Beach. **(C)** View southwest along the lagoon-side beach of the McLoughlins Beach barrier, toward Nooramunga Midden. **(D)** View northeast toward McLoughlins Channel with the footbridge and McLoughlins Beach township visible.

aligned along a bearing of 212° to follow the orientation of the dune edge. This location was chosen to encompass a small concentration of eroding shells in a dark brown-gray sediment horizon. This dark brown-gray sediment horizon and the lens of eroding archaeological shells were less dense than in the McLoughlins Beach 1 excavation 200 m away. Due to this reduced frequency and density of archaeological remains, the excavation team aimed to determine if the entire length of the midden complex (registered in their entirety as Nooramunga Midden) was contemporaneous. Further, McLoughlins Beach 2 was laid in this location as a distinctive, dense lower shell layer was also visible in the dune profile. This lower layer was characterized by coarse sediments, including water-rolled

pebbles, and a range of water-rounded shell taxa that included small individuals of species not previously known to have been targeted by people in the past in this region. The shell from this lower layer was broken and slightly edge-rounded, and had the appearance of a natural shell deposit (Figure 3).

Excavations were conducted in 2 cm arbitrary excavation units (XUs) or spits oriented to follow stratigraphic units (SUs) or layers. Bulk sediment samples were taken from each XU. Excavated sediments were dry-sieved through 2 mm mesh sieves and all materials retained in the sieves were transported to the Monash Indigenous Studies Centre

FIGURE 2
Environmental context at McLoughlins Beach barrier dune system. **(A)** Aerial view toward the barrier system lagoon-side beach. **(B)** View from the lagoon-side dunes to McLoughlins Channel and footbridge. **(C)** View southwest along the lagoon beach, indicating the extensive seagrass beds and seagrass wrack at low tide. **(D)** Aerial view of the exposed ocean-side of the barrier system (Ninety-Mile Beach). **(E)** Ground view southwest along the exposed Ninety-Mile Beach. **(F)** Barrier system interior vegetation.
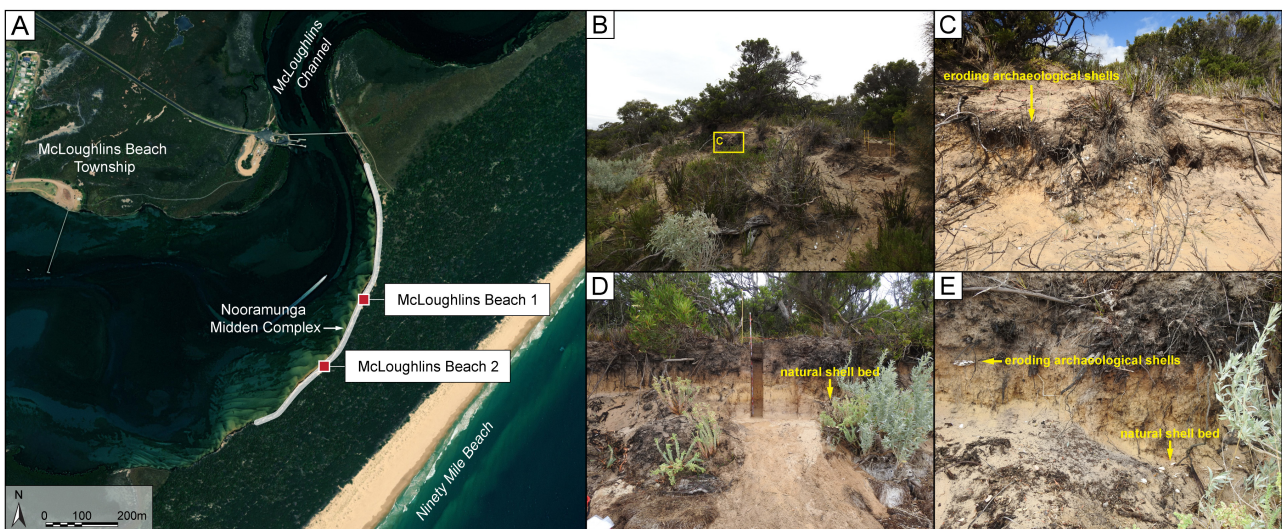

FIGURE 3
The archaeological sites. **(A)** Map indicating the location of the McLoughlins Beach 1 and McLoughlins Beach 2 excavations in relation to Nooramunga Midden Complex. **(B)** View toward Nooramunga Midden Complex, with McLoughlins Beach 1 excavation visible to the right. **(C)** Close view of eroding shell remains and charcoal rich gray lens near McLoughlins Beach 1. **(D)** View toward McLoughlins Beach 2 excavation. **(E)** Clump of eroding shells and natural shell bed visible in the dune profile at McLoughlins Beach 2 prior to excavation.

archaeology laboratory, Monash University, Australia, for sorting and analysis.

Nine radiocarbon age determinations were obtained from the McLoughlins Beach 1 excavation (Table 1). Six of these radiocarbon ages were on single pieces of unidentified charcoal and three were on marine shell. The habitat and diet of the molluscan taxa sampled for dating can significantly impact the radiocarbon ages. The bivalve *Latona deltoides* was selected for analysis because it is an open-ocean taxon (as opposed to estuarine) that lives in sandy substrates on wave-dominated

TABLE 1 AMS radiocarbon age determinations for McLoughlins Beach 1 and 2 excavations.

Lab ID	XU	SU	Sample material	Sample weight (g)	δ^{13}C (‰)	Conv. ^{14}C Age (BP)	Calibrated age (cal BP)		
							68.3% prob.	95.4% prob.	Median
McLoughlins Beach 1									
Wk-56443	15	1C	Charcoal	0.11		129 ± 16	250–20	260–0	80
Wk-56444	19	2	Charcoal	0.02		673 ± 16	650–550	660–550	600
Wk-56700	22	2	Marine shell *Latona deltoides*	0.61	0.4 ± 0.6	1,038 ± 21	630–520	680–460	580
Wk-56445	23	2	Charcoal	0.33		588 ± 16	560–530	630–520	540
Wk-56446	24	2	Charcoal	0.07		882 ± 17	770–720	800–680	740
Wk-56701	26	3	Marine shell *Latona deltoides*	0.95	−1.4 ± 0.6	1,596 ± 20	1,200–1,040	1,260–970	1,120
Wk-56699	28	3	Marine shell *Latona deltoides*	0.58	−1.8 ± 0.6	2,016 ± 20	1,630–1,460	1,700–1,390	1,550
Wk-56447	28	3	Charcoal	0.34		1,864 ± 15	1,810–1,710	1,820–1,700	1,750
Wk-56448	36	4	Charcoal	0.10		1,135 ± 15	1,050–950	1,060–930	990
McLoughlins Beach 2									
Wk-56453	11	5	Charcoal	0.11		1,119 ± 16	1,050–930	1,050–930	970
Wk-56450	15	5	Marine shell *Latona deltoides*	4.53		1,708 ± 17	1,300–1,160	1,350–1,080	1,230
Wk-56703	25	6	Marine shell *Latona deltoides*	0.86		3,999 ± 22	4,080–3,900	4,260–3,810	3,990
Wk-56451	27	7	Marine shell *Dosinia caerulea*	10.16		3,625 ± 17	3,580–3,420	3,670–3,360	3,500
Wk-56452	27	7	Marine shell *Austromactra rufescens*	6.76	1.9 ± 0.3	36,291 ± 417	40,850–40,050	41,200–39,700	40,450

Age calibrations were conducted in OxCal v4.4 (Bronk Ramsey, 2009) using the SHCal20 atmospheric curve (Hogg et al., 2020) for charcoal and the Marine20 (Heaton et al., 2020) curve for marine shell samples. The calibrated ages on the shell used a ΔR value of −123 ± 22 years, from eight marine shells obtained between Wilsons Promontory and Lakes Entrance, as presented in Ulm et al. (2023).

beaches (Boyd, 2011). Three of the charcoal samples were collected *in situ* from XU23, XU24, and XU28. Three charcoal samples were obtained from the sieve from XU15, XU19, and XU36. The three radiocarbon determinations obtained from *Latona deltoides* shell valves were taken from the sieve from XU22, XU26, and XU28. Five radiocarbon determinations were obtained from McLoughlins Beach 2 (Table 1). One is on an individual piece of charcoal, the other four on marine shell. The charcoal sample was collected *in situ* from the northeast profile. Three of the marine shell samples were also collected *in situ*—two from the southeast profile and one from the northeast profile. One marine shell was collected from the sieve in XU25 (Table 1). See Supplementary file for details of radiocarbon dating procedures.

Molluscs were the primary component of the excavations and were identified to their lowest taxonomic level using identification manuals, published literature (Boyd, 2011; Heldt and Mayfield, 2020) and an eastern Australia marine fauna reference collection held at the Monash Indigenous Studies Centre archaeology laboratory. Taxonomic nomenclature was verified using the World Register of Marine Species online database (WoRMS Editorial Board, 2024). Following discipline conventions, mollusc remains were quantified using Minimum Number of Individuals (MNI; Harris et al., 2015), Number of Identified Specimens (NISP; Reitz and Wing, 2008), and weight rounded to the nearest 0.01 g.

4 Results

4.1 Geomorphology of the Nooramunga Midden Complex

4.1.1 Surficial geomorphology

The wider landscape setting on which the midden complex is found is a regressive barrier spit, principally composed of a series of parallel (up to 10) foredune ridges that can be traced as continuous features for kilometers along the spit to form a plain around 240 m wide (Figure 4). This ridge-plain is attached to the hinterland 5.5 km north of the midden complex near Reeves Beach. The foredune ridge landscape ranges from 4 to 5 m above MSL.

On the estuary (landward) side of the foredune ridge-plain, a distinct higher ridge reaches over 7 m in elevation. This single ridge extends almost 1.5 km along the back of the spit from its southern extent. This ridge is over 30 m wide, and in places appears to have formed on top of older linear foredune ridges of the main part of the spit. The ridge extends as a linear feature 1.7 km from the southern tip of the barrier, where it is interrupted by parabolic depressions 480 m south of the McLoughlins Beach 2 excavation. A ridge extends northward as a single crest (from 20 m northward of McLoughlins Beach 1) as a hummocky dune ridge with a relief of around 5 m extending up to 7 m above MSL (Figure 5). It is, however, absent from a 630 m section of the estuarine coast at the center of the site, where the McLoughlins Channel has eroded into the barrier sequence. The hummocky dune ridge, especially at its northern end, is dissected by many troughs and blow-out features orientated perpendicular to the shoreline, all of which are currently fully vegetated and therefore stable, with little aeolian sediment transport currently occurring. The ridge is separated from

the foredune-ridge part of the main barrier complex by a swale up to 160 m wide, which lies between 2.6 and 4.0 m above MSL (Figure 5). The swale is a maximum width of 160 m at the northern end of the site, and a minimum of 20.1 m wide at the location of the McLoughlins Beach 2 excavation. It is within the exposed part of the swale, where the hummocky dune ridge is absent, that the archaeological investigations were undertaken (Figure 4).

4.2 Radiocarbon and OSL chronology of Nooramunga Midden Complex

4.2.1 McLoughlins beach 1

McLoughlins Beach 1 was excavated to a maximum depth of 135.7 cm, with the top of the excavation being 3.59 m above MSL. Four distinct stratigraphic units (SUs) were identified, SU1 and SU4 each containing sub-SUs (see Supplementary file). Directly next to the base of the excavation an auger hole was cored to a depth of 2.80 m (0.79 m above MSL).

Nine radiocarbon (Table 1) and two OSL (Table 2) age determinations were obtained from McLoughlins Beach 1. One of the OSL samples was taken horizontally into the excavation face 0.3 m below its top in XU9 and XU10, the second at the base of the auger hole between 2.56 and 2.80 m below the excavation surface (0.79–1.03 m elevation above MSL). Table 2 provides a summary of the environmental dose rates, single-grain D_e values and final ages for the two OSL dating samples (MLB1 and MLB2) from the McLoughlins Beach 1 excavation pit. The single-grain D_e distributions of grains that passed the SAR quality assurance criteria are shown as radial plots in Figure 6. Both samples exhibit homogenous single-grain OSL D_e distributions that are consistent with well-bleached, unmixed sediments (e.g., Arnold et al., 2008, 2016; Jacobs et al., 2016; Arnold and Roberts, 2009; Bailey and Arnold, 2006; Demuro et al., 2023). The single-grain OSL dataset of sample MLB2 displays a low relative overdispersion value of 23 ± 2% (Table 2). MLB1 exhibits a higher relative overdispersion value of 57 ± 8%, however this is primarily a reflection of the very low natural D_e values obtained for this sample (ranging from −0.6 ± 0.3 Gy to 1.4 ± 1.0 Gy). When expressed in absolute terms (i.e., Gy instead of %), this sample exhibits a very small overdispersion value of 0.06 ± 0.01 Gy. These overdispersion values are consistent with (i.e., within 2σ of) those typically reported for well-bleached and undisturbed single-grain D_e datasets (e.g., average relative overdispersion values of 20 ± 1% to 30 ± 1% obtained for Holocene and Pleistocene samples by Arnold and Roberts, 2009, and Arnold et al., 2022; average absolute overdispersion value of 0.12 ± 0.05 Gy obtained for modern and very-young samples by Arnold et al., 2019). Application of the maximum log likelihood (L_{max}) test (Arnold et al., 2009) indicates that the central age model (CAM) is statistically favored over the three- or four-parameter minimum age models (MAM-3 or MAM-4) of Galbraith et al. (1999) for the two D_e datasets. We have therefore used the weighted mean (CAM) D_e values to derive the final OSL burial dose estimates for samples MLB1 and MLB2, in accordance with the L_{max} test results (Arnold et al., 2009; Table 2). As sample MLB1 contains near-zero Gy and negative D_e values (overlapping with 0 Gy at 2σ), it was necessary
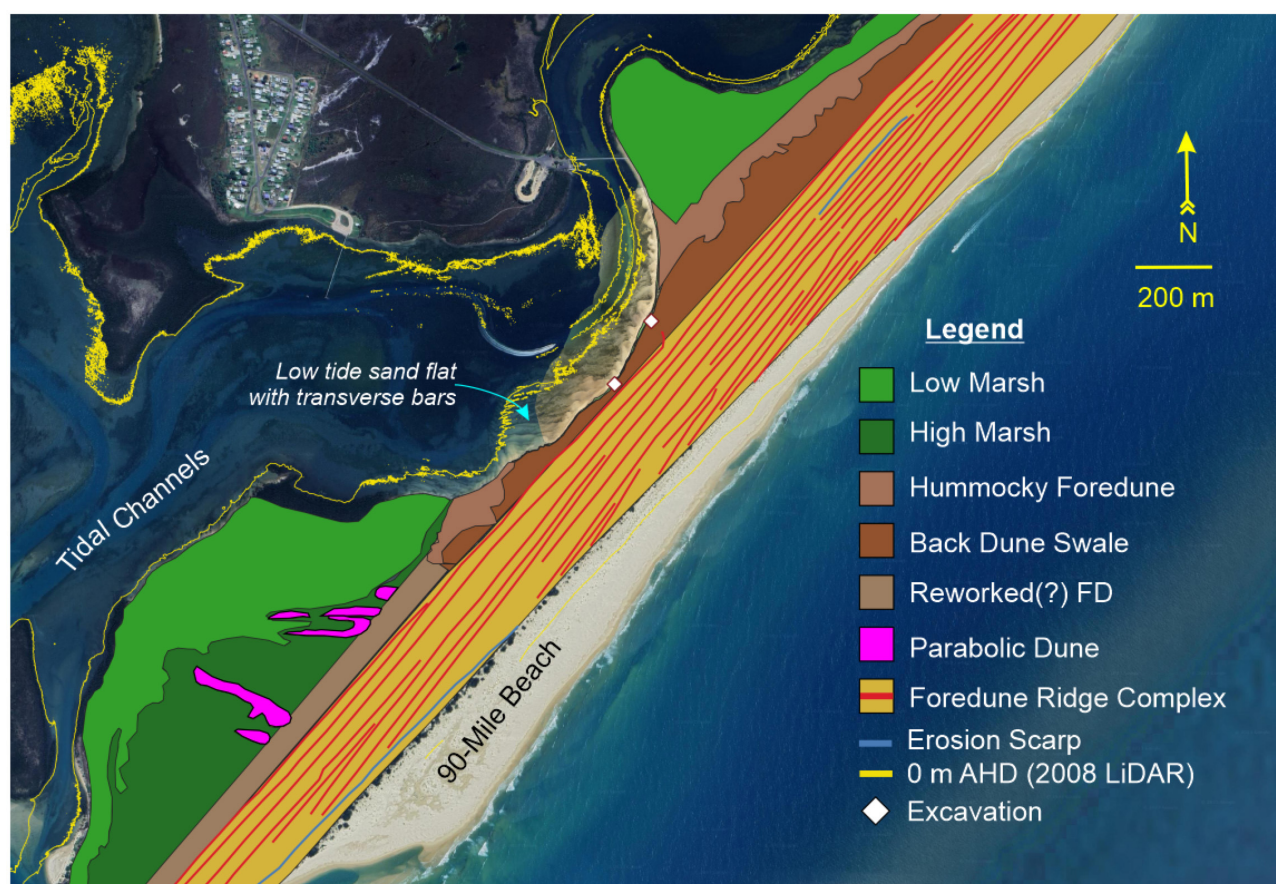
FIGURE 4
Geomorphic map of the wider landscape setting in which the archaeological excavations were undertaken. The middens are found within a swale at the landward side of a small plain composed of prograded foredune ridges.

to apply the unlogged version of the central age model (CAM_{UL}) to this dataset.

The calibrated radiocarbon results (at 95.4% probability) indicate that SU1, comprised of aeolian sand, built up over the past few 100 years (Wk-56443: 260–0 cal BP at the base of SU1C). This young age is further supported by a single-grain OSL age of 0.13 ± 0.01 ka (1σ uncertainty) in the center of SU1C (Table 2). SU2, containing archaeological remains (charcoal, shell, stone artifacts, bone), dates from 800–680 cal BP (Wk-56446) to c. 520 cal BP (Wk-56444: 660–550 cal BP; Wk-56445: 630–520 cal BP). This layer has the dispersed remains of multiple campfires (as indicated by the high abundance of charcoal) and shell. SU3 dates from 1,820 cal BP (Wk-56447) to 970 cal BP (Wk-56701). An additional calibrated radiocarbon age of 1,700–1,390 cal BP (Wk-56699) also comes from this period of occupation. It, too, is associated with charcoal and shell (Table 1). A radiocarbon age on charcoal from the base of SU4B dates to 1,060–930 cal BP (Wk-56448). This piece of charcoal was obtained from the sieve. It is the lowermost charcoal from the deposit and is thought to have post-depositionally moved down in the sand dune from higher up, or during the excavation due to the windy, rainy conditions experienced at the time of this XU's excavation (Table 1; Figures 7, 8). SU4 contains minimal charcoal (weight = 1.59 g) and mollusc shell (weight = 2.22 g; NISP = 102;

see Supplementary Table S4.2) which, due to the anomalous date (Wk-56448), is currently undated. Below the base of the excavation, the fine, well-sorted sand extended a further 56 cm in depth, where it encountered a c. 30 cm-thick gravelly shell deposit that overlay a fine sandy sequence. These two sediment horizons are equivalent to SU7 and SU8 in the McLoughlins Beach 2 excavation described below. A single-grain OSL age of 2.17 ± 0.13 ka was obtained from the base of the auger hole, equivalent in age to SU8 in the McLoughlins Beach 2 excavation (Table 2).

4.2.2 McLoughlins beach 2

McLoughlins Beach 2 was excavated to a maximum depth of 146.3 cm, with the excavation top occurring at an elevation of 3.58 m above MSL. Eight distinct SUs were identified (see Supplementary file). Five radiocarbon determinations were obtained from McLoughlins Beach 2 (Table 1). The calibrated age results (at 95.4% probability) indicate that SU5, containing archaeological remains (charcoal, shell), was occupied from 1,350 cal BP (Wk-56450) to 930 cal BP (Wk-56453). The age of the base of SU5 (Wk-56450: 1,350–1,080 cal BP) was obtained on shell from the clump of eroding shells visible in the dune profile
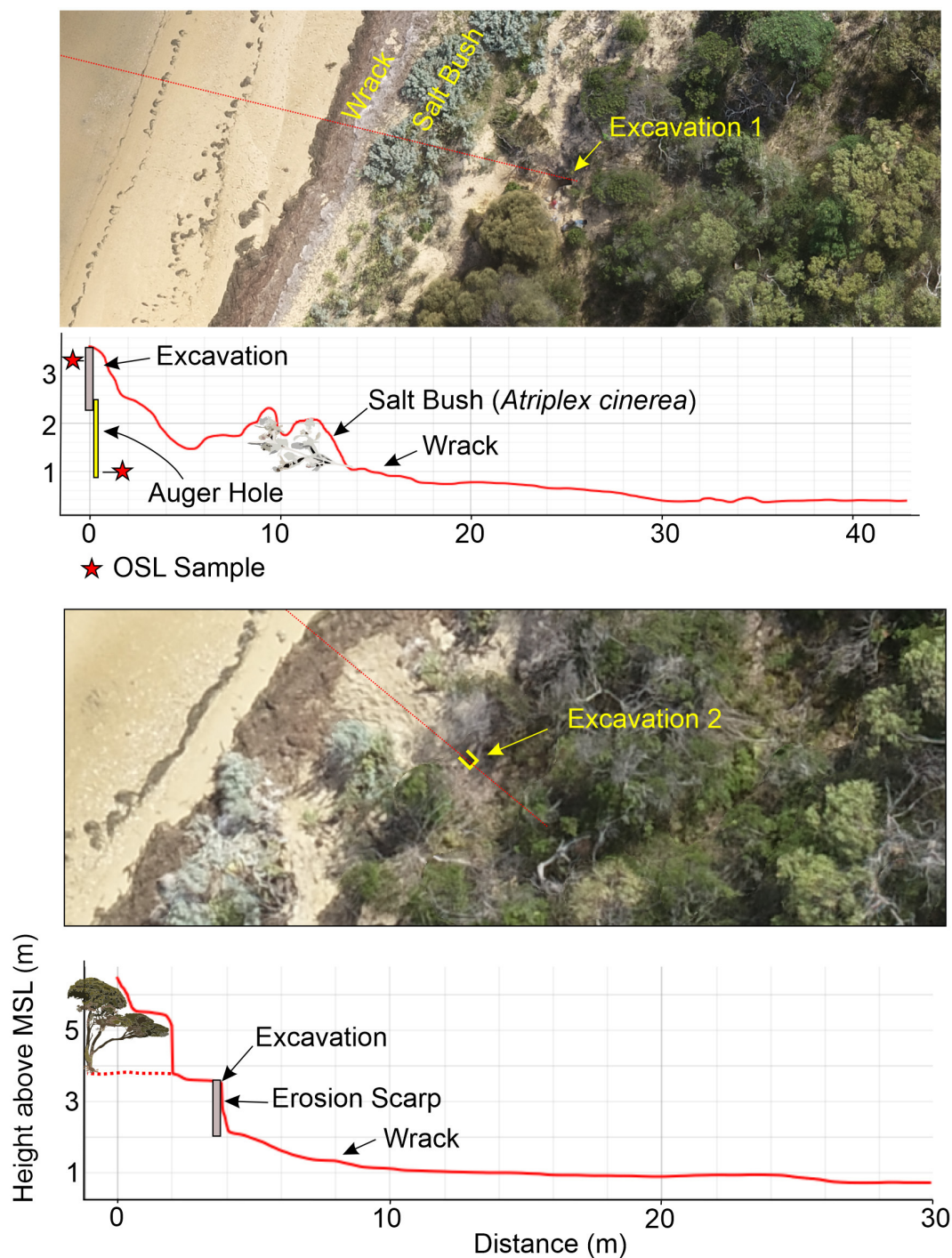
FIGURE 5
An aerial view of McLoughlins Beach 1 **(top)** and McLoughlins Beach 2 **(bottom)** excavations and their relationship to mean sea level. The profile is derived from a digital surface model and therefore represents both the land and vegetation surface.

prior to excavation (Figure 3E). These results indicate that SU5 at McLoughlins Beach 2 is contemporaneous with SU3 (the lower occupation layer) at McLoughlins Beach 1. This suggests that the upper midden horizon (the more recent occupation levels) evident at McLoughlins Beach 1 (SU2: 800 to 460 cal BP) is absent (perhaps lost through erosion) at McLoughlins Beach 2. At McLoughlins Beach 2, radiocarbon ages on marine shell from the coarse sand and pebble layer at the bottom of the deposit (SU7) dates between 4,260 and 3,360 cal BP (Wk-56703: 4,260–3,810 cal BP; Wk-56451: 3,670–3,360 cal BP). An anomalous radiocarbon age of 41,200–39,700 cal BP was also obtained (Wk-56452) from this water-rolled shell, coarse sand and pebble horizon, likely reworked older near-shore submarine deposits (Table 1; Figures 7, 8).

TABLE 2 Summary of environmental dose rates, D_e data and final ages for the OSL dating samples from McLoughlins Beach, both taken from McLoughlins Beach 1 archaeological excavation.

Sample	Depth (m)	Water content (%)[a]	Environmental dose rate (Gy/ka)					Equivalent dose (D_e) data				Age (ka)[e,i]
			Beta dose rate[b]	Gamma dose rate[b]	Cosmic dose rate[c]	Internal dose rate[d]	Total dose rate[e]	No. of grains[f]	OD (%)[g]	Age model[h]	D_e (Gy)[e]	
MLB1	0.3	0.2 ± 0.1	0.39 ± 0.02	0.20 ± 0.01	0.20 ± 0.02	0.03 ± 0.01	0.82 ± 0.04	167/800	57 ± 8	CAM$_{UL}$	0.11 ± 0.01	0.13 ± 0.01
MLB2	2.7	2.5 ± 1.2	0.42 ± 0.02	0.26 ± 0.02	0.15 ± 0.02	0.03 ± 0.01	0.86 ± 0.04	145/800	23 ± 2	CAM	1.87 ± 0.05	2.17 ± 0.13

[a] Long-term estimated water content, expressed as % of dry mass of mineral fraction, with an assigned 1σ uncertainty of ±50%. The long-term water contents of these samples are taken as equivalent to the present-day water contents.

[b] Beta and gamma dose rates have been determined from dried and powdered bulk sediment samples using high-resolution gamma spectrometry. Beta dose rates have been calculated after making allowance for beta dose attenuation due to grain-size effects and HF etching (Mejdahl, 1979; Brennan, 2003). Specific activities and radionuclide concentrations have been converted to dose rates using the conversion factors given in Guérin et al. (2011).

[c] Cosmic-ray dose rates were calculated according to Prescott and Hutton (1994) and assigned a relative 1σ uncertainty of ± 10%.

[d] The assumed internal alpha and beta dose rate for quartz, with an assigned relative 1σ uncertainty of ±30%, is based on intrinsic ^{238}U and ^{232}Th contents published by Mejdahl (1987), Bowler et al. (2003) Jacobs et al. (2006), Pawley et al. (2008), and Lewis et al. (2020), and an a-value of 0.04 ± 0.01 (Rees-Jones, 1995; Rees-Jones and Tite, 1997). Intrinsic radionuclide concentrations and specific activities have been converted to dose rates using the factors given in Guérin et al. (2011), making allowance for beta dose attenuation due to grain-size effects (Mejdahl, 1979).

[e] Mean ± total uncertainty (68% confidence interval), calculated as the quadratic sum of the random and systematic uncertainties.

[f] Number of D_e measurements that passed the SAR rejection criteria and were used for D_e determination/total number of D_e values analyzed.

[g] OD, overdispersion, which equates to the relative spread in the D_e dataset beyond that associated with the measurement uncertainties for individual D_e values.

[h] CAM, central age model (Galbraith et al., 1999); CAM$_{UL}$, unlogged central age model (Arnold et al., 2009). Sample MLB1 contained near zero Gy and negative D_e values (overlapping with 0 Gy at 2σ), and therefore it was necessary to apply the CAM$_{UL}$ to this dataset.

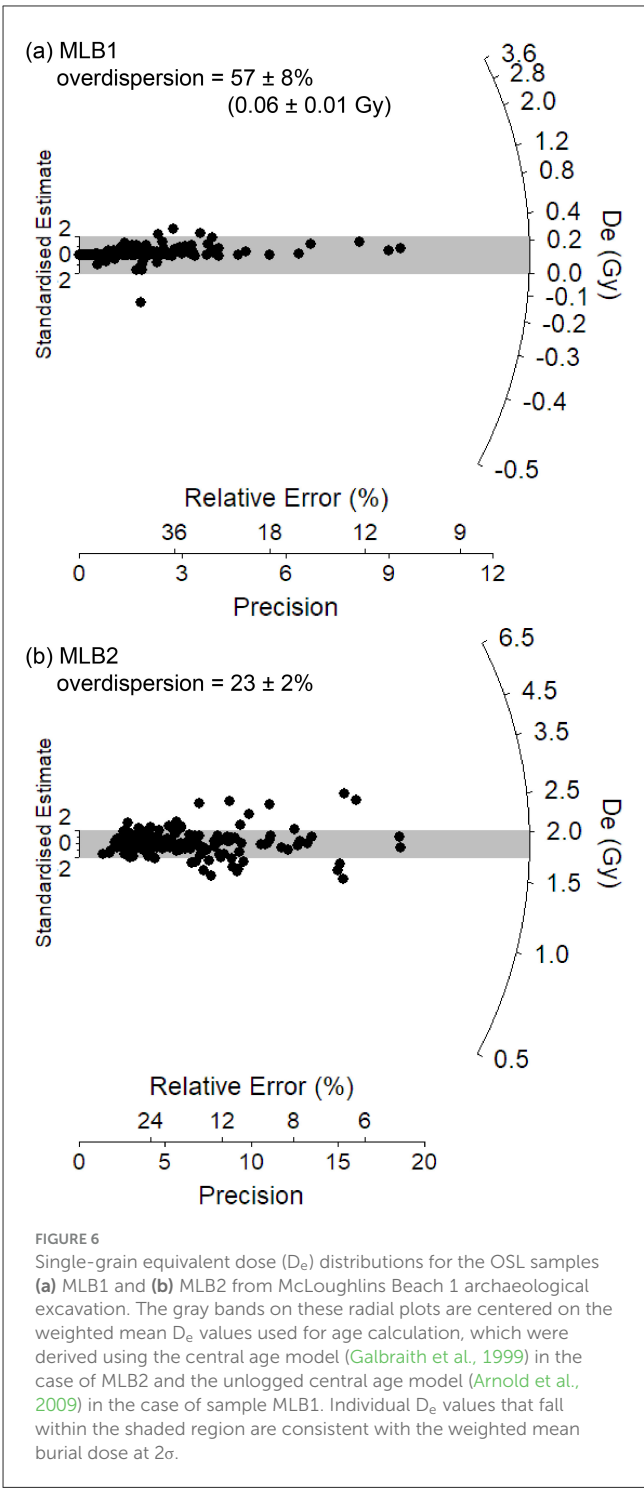[i] Total uncertainty includes a systematic component of ±2% associated with laboratory beta-source calibration.

FIGURE 6
Single-grain equivalent dose (D_e) distributions for the OSL samples (a) MLB1 and (b) MLB2 from McLoughlins Beach 1 archaeological excavation. The gray bands on these radial plots are centered on the weighted mean D_e values used for age calculation, which were derived using the central age model (Galbraith et al., 1999) in the case of MLB2 and the unlogged central age model (Arnold et al., 2009) in the case of sample MLB1. Individual D_e values that fall within the shaded region are consistent with the weighted mean burial dose at 2σ.

4.3 Mollusc identification and quantification

At McLoughlins Beach 1, marine shell was the primary constituent of the midden horizons, with a total MNI of 161 and NISP of 3828 (703.5 g; 82.2% of cultural materials by weight; Figures 7, 8; Supplementary file). The shell mainly came from SU2 (234.3 g; 33.3%) and SU3 (466.7 g; 66.3%). A very small shell

assemblage was also present in SU4 (2.2 g; 0.3%). SU2 contains an MNI of 75 (46.3%) and NISP of 2,159 (56.4%), and SU3 an MNI of 85 (52.5%) and NISP of 1,547 (40.4%). SU4 has an MNI of 1 (0.6%) and NISP of 102 (2.7%). In both SU2 and SU3, the identified taxa are *Anapella cycladea*, *Katelysia* spp. and *Latona deltoides*. In SU4, the single identified taxon is *Latona deltoides* (Figure 9). The vertical variation in taxonomic abundance through SU2, SU3, and SU4 indicates a change in the range and intensity of shellfish gathering through time (Figure 10). Initially, people gathered *L. deltoides*, being the dominant taxon in both SU4 (MNI = 1; 100%) and SU3 (MNI = 46; 54.1%). *Katelysia* spp. was also a major contributing taxon in SU3 (MNI = 36; 42.4%), with a small contribution of *A. cycladea* (MNI = 2; 2.35%). Then, in SU2, *A. cycladea* became the dominant taxon (MNI = 34; 45.3%), with smaller contributions from both *L. deltoides* (MNI = 17; 22.7%) and *Katelysia* spp. (MNI = 22; 29.3%; Figure 10; Supplementary file).

Latona deltoides lives in sandy substrates in wave-dominated beaches that are exposed, high energy environments. *Katelysia* spp. instead occupies sheltered, low energy environments such as estuaries and sandflats primarily in sand and can tolerate some muddy sediments. *Anapella cycladea* also occupies sheltered, low energy environments such as estuaries on mudflats and can live in sand and mud (Boyd, 2011; Heldt and Hart, 2021; Heldt and Mayfield, 2020). Taxonomic changes through time indicate that people were initially foraging along high energy, exposed surf beaches, with increasing foraging along sheltered (low energy) estuaries through time up through the deposit, until the low energy muddy habitats became the dominant environment represented. There is an increase in taxa that can occupy mudflats and muddy sediments through time (Figure 10).

Marine shell is the primary cultural constituent of the McLoughlins Beach 2 midden, with a total MNI of six and NISP of 148 (46.9 g; 66.5% of cultural materials by weight; Figures 8, 9). SU5 has a mollusc MNI of six (100%) and NISP of 104 (67.1%). Identified archaeological mollusc remains at McLoughlins Beach 2 almost entirely consist of *Latona deltoides*, with one c.f. *Katelysia* sp. fragment from XU3 possibly being more recent (Figure 8; Supplementary file). The lower natural shell bed contains a range of water-rolled marine mollusc taxa including *Dosinia caerulea*, *Austromactra rufescens*, *Ostrea angasi*, *Anadara trapezia*, *Glycymeris radians*, and *Pecten fumatus*, as well as unidentified water-rounded shell grit and water-rounded beach rock.

5 Discussion and conclusion

Excavation of McLoughlins Beach 1 and McLoughlins Beach 2 at Nooramunga Midden revealed c. 1,300 years of repeated camping, from c. 1,820 cal BP to 520 cal BP (Wk-56447, Wk-56445 at 95.4% probability; Table 1). Shellfish were gathered along high-energy, exposed surf beaches and from low-energy, sheltered estuaries with associated mudflat environments. There is minimal evidence of people also using stone tools and consuming terrestrial animals on the dune (Figure 8). Given both the high density and spatial extent of the Nooramunga Midden Complex, and the contemporaneity of the SU3 horizon at McLoughlins Beach 1 (lower, i.e., earlier phase of occupation) and SU5 at McLoughlins

Beach 2, it is likely that reasonably large (family) groups of people came to this area together to camp and gather shellfish (Bowdler, 1976; Meehan, 1982).

At McLoughlins Beach 1, the change in relative abundance of shell taxa and their targeted associated habitats through time is notable (Figures 7–10). It appears that these changes represent a rapidly transforming landscape around Nooramunga Midden. Here, we describe a preliminary geomorphic sequence for the McLoughlins Beach barrier system (Figure 11). This chronological sequence was developed through the coastal geomorphic and archaeological data reported here and previous luminescence dating of the seaward foredune ridges reported in Kennedy et al. (2020).

Stage 1 represents the period when this area of Nooramunga Marine and Coastal Park began to transform from an open coast embayment to a semi-enclosed lagoon behind a series of low sand islands dominated by overwash. The timing of overwash development is constrained by the lowest elevation age (+0.79 m above MSL) across the barrier taken from the sand unit (SU8) below the coarse shelly sediment (SU7). This indicates deposition of an intertidal surface 2.17 ± 0.13 ka. The formation of the intertidal island was likely rapid and of similar width to the contemporary barrier based on the age structure of the barrier beneath the seaward linear foredune ridges. Dating of the dune scarp on the open ocean side of the beach reveals ages of between 1.77 ± 0.9 and 1.84 ± 0.8 ka (Kennedy et al., 2020). The lowest elevation age for the foredune barrier complex from this earlier work is at +1.5 m on the oceanward-facing dune scarp, 26 cm higher than our age from the McLoughlins Beach 2 excavation.

Stage 2 represents a period of hardening of the intertidal sand island, through overwash deposition of a layer of shells and beach-rock gravel. This period is exposed in the McLoughlins Beach 2 excavation and sampled in the auger hole below the McLoughlins Beach 1 excavation. Three radiocarbon ages from this horizon are, however, much older than those returned above and below them, with one c. 40,450 cal BP (Wk-56452) and two between 4,260 and 3,360 cal BP (Wk-56703, Wk-56451). The dated samples were broken shell fragments and were likely transported to the site by marine processes. They therefore represent reworking of shallow marine sediment, associated with a change in the hydrodynamics of the now developing estuarine lagoon forming behind the developing sandy island. This shell deposit likely provided some stability to the newly emerged island over which dunes could form, similar to the prograding barrier of Farewell Spit in New Zealand today (Tribe and Kennedy, 2010). During Stage 2, the lagoon area remained open and under the influence of tides and locally generated wind waves. This means that the *Latona deltoides* habitats would have been extensive along both sides of the island that later became the McLoughlins Beach dune barrier. Previously, the low, wave-overwash island may have been too continuously inundated for *L. deltoides* to grow, as the species prefers intertidal (rather than subtidal) conditions; it does not fare well in permanently submerged conditions (Figure 11).

In Stage 3, the low elevation sandy island rapidly transformed into a wide barrier island plain as the shoreline rose in height to form foredunes, which subsequently prograded seaward at a rate of 0.64 m/yr. Deposition of these ridges appears to have been
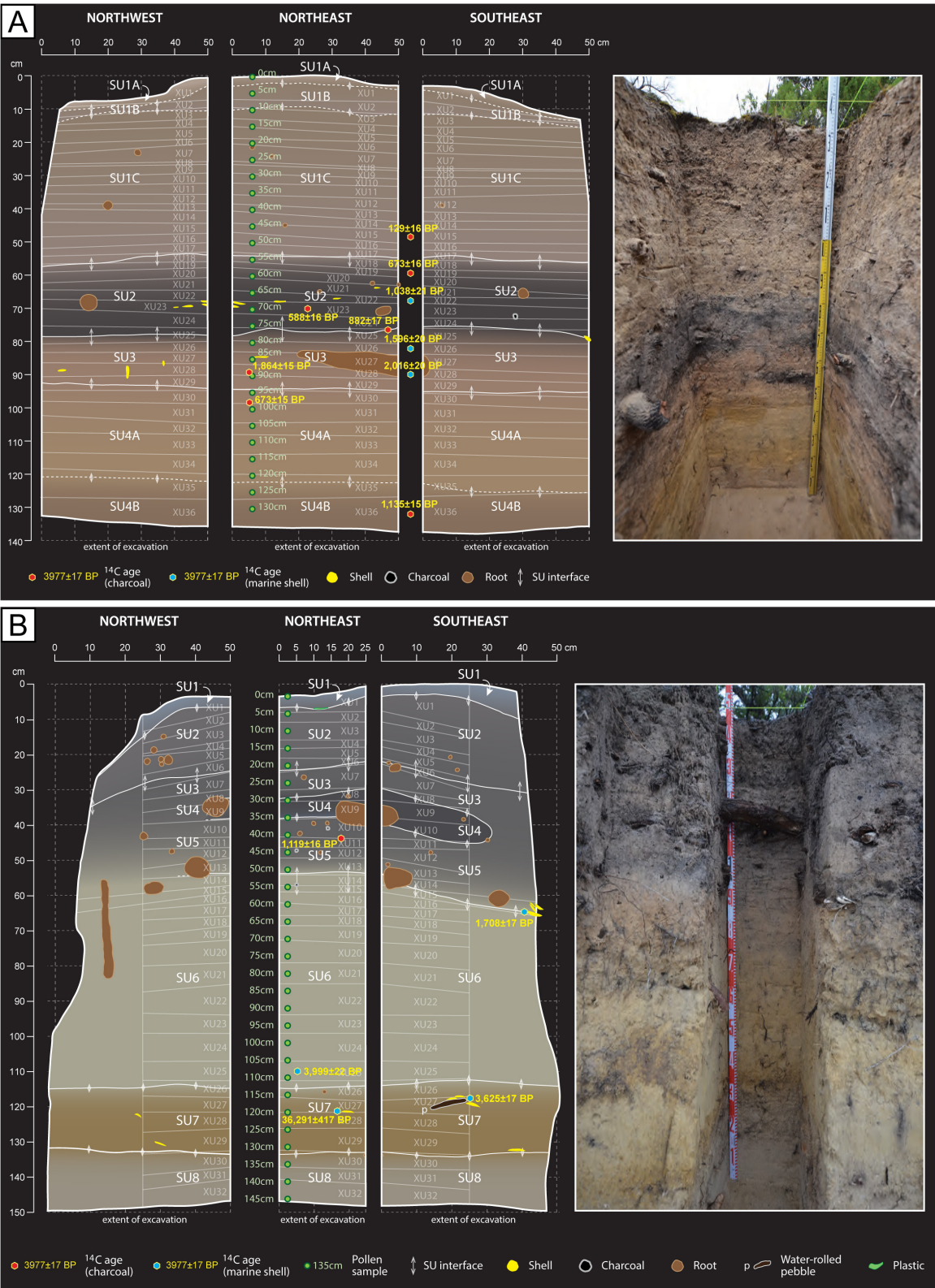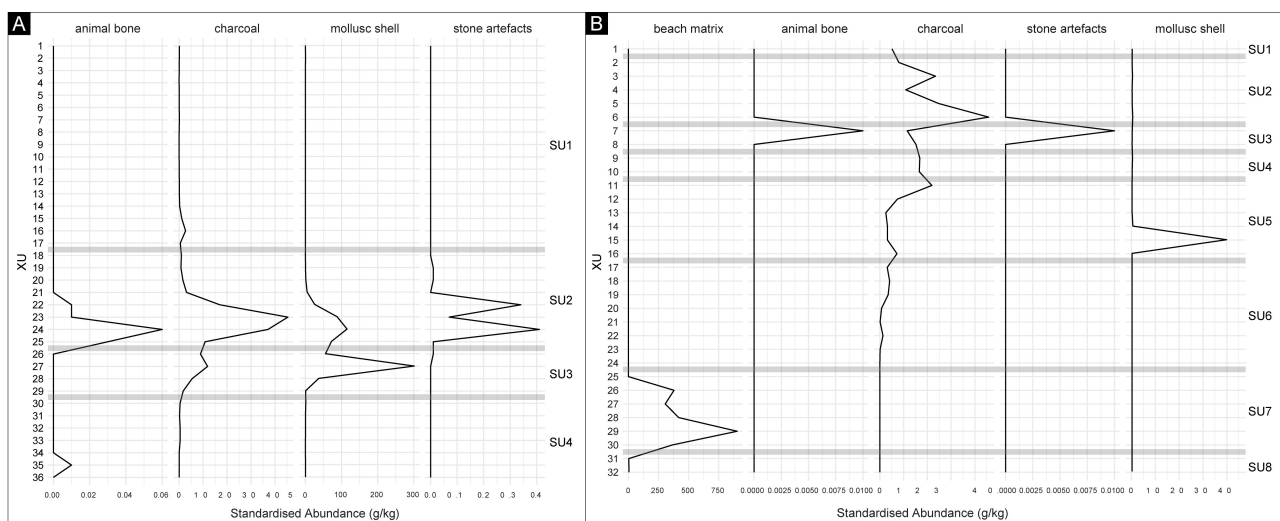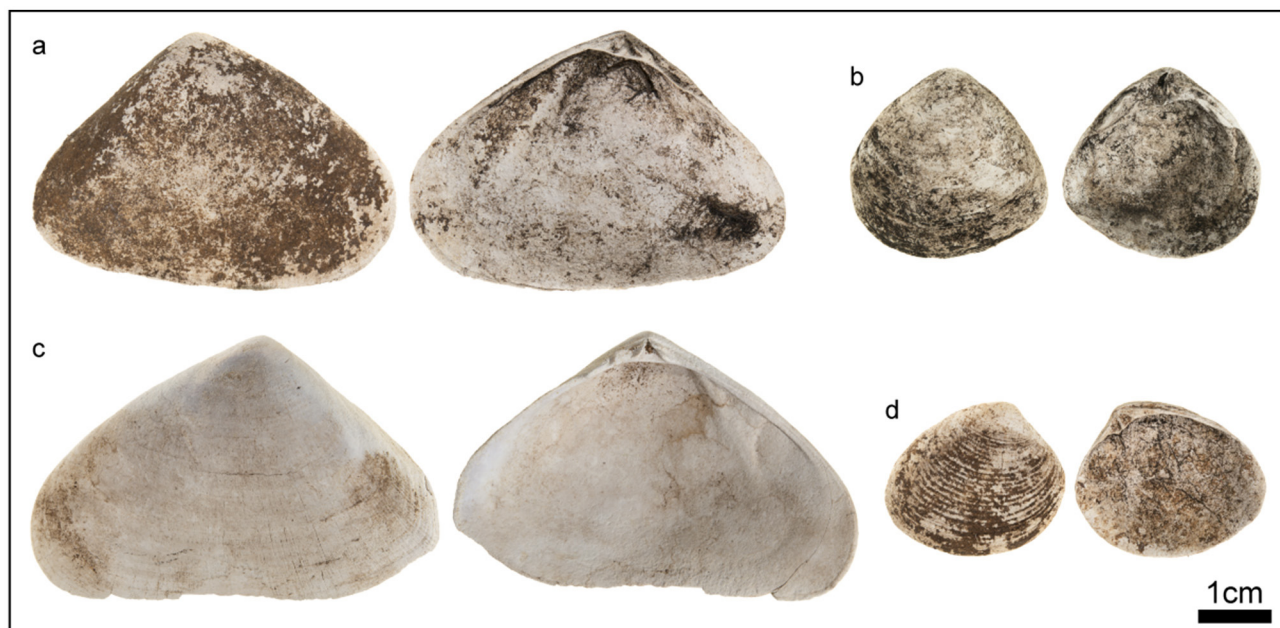
FIGURE 7
Section drawings after completion of excavations. **(A)** McLoughlins Beach 1 section drawing with uncalibrated radiocarbon ages projected. **(B)** McLoughlins Beach 2 section drawing with uncalibrated radiocarbon ages projected. See Table 1 for calibrated ages.

FIGURE 8
Standardized abundance plots (in grams of archaeological materials per kilogram of excavated sediment), by XU. (A) McLoughlins Beach 1. (B) McLoughlins Beach 2. The horizontal gray lines indicate the depth and thickness of the interfaces between SUs.
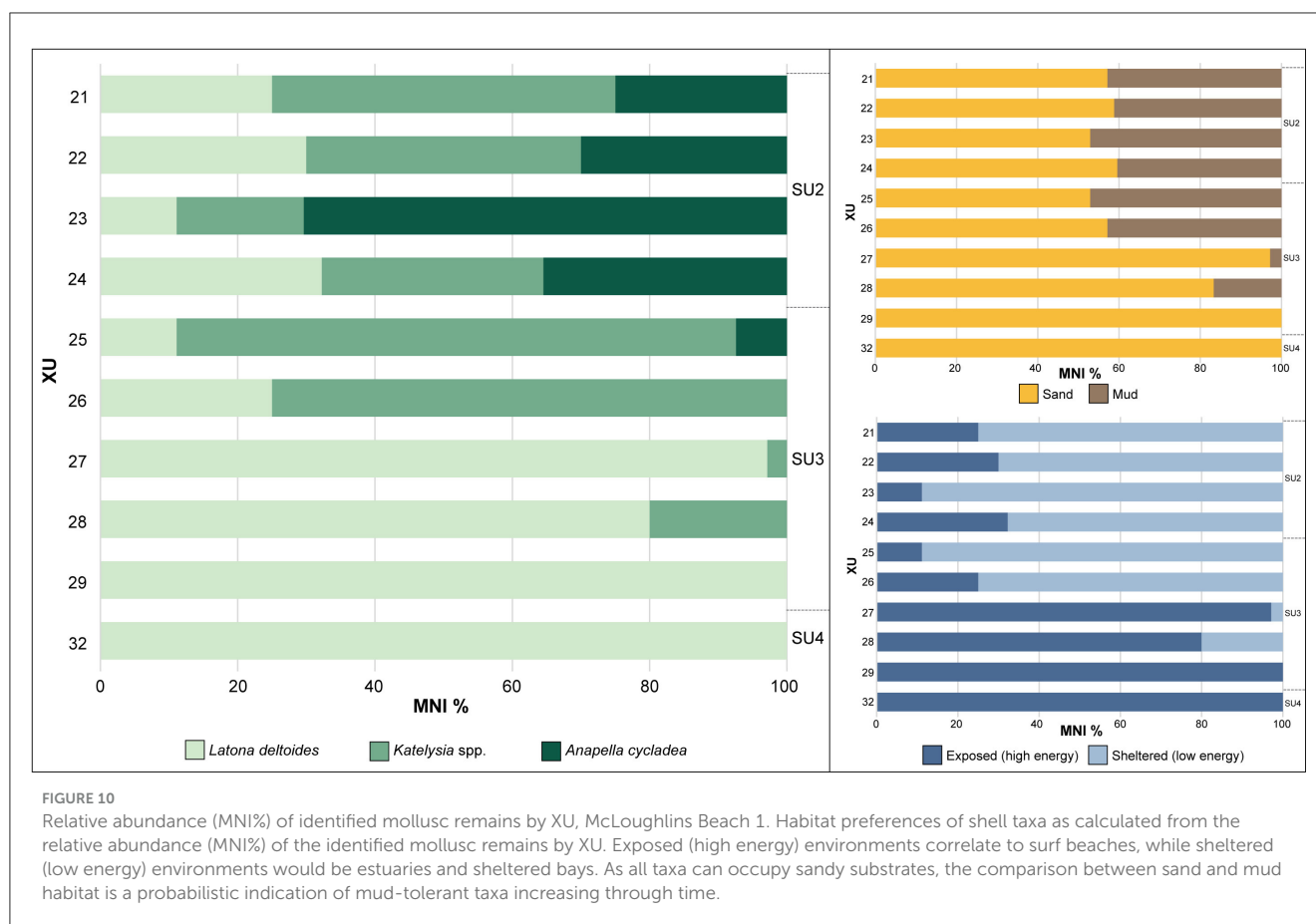

FIGURE 9
Examples of excavated shell remains from McLoughlins Beach 1 and McLoughlins Beach 2: (a) *Latona deltoides* from McLoughlins Beach 1, XU27. (b) *Anapella cycladea* from McLoughlins Beach 1, XU22. (c) *Latona deltoides* from McLoughlins Beach 2, XU15. (d) *Katelysia* spp. from McLoughlins Beach 1, XU27.

near-concurrent with the development of the island foundation, dating between 2.38 ± 1.1 ka and 2.17 ± 1.0 (Kennedy et al., 2020). These ages of ridges from the central part of the barrier are several 100 years older than the lower-elevation samples on the barrier edge, which suggests concurrent lateral extension of the intertidal sand flats as the dunes built seaward.

Stage 3 also represents a period of estuary formation, as indicated by the initial stages of infill. The distance across the island (i.e., across the then-active barrier dune system) from its lagoon-side to the open ocean increased due to barrier elongation and widening. Locally generated wind waves around the lagoon continued. This stage is also when people began to visit the McLoughlins Beach barrier, and dates to sometime between 1,820 and 1,390 years ago (Wk-56447, Wk-56699 at 95.4% probability). They foraged for *L. deltoides* in high-energy, surf beach environments that were present on the ocean-side of the

FIGURE 10
Relative abundance (MNI%) of identified mollusc remains by XU, McLoughlins Beach 1. Habitat preferences of shell taxa as calculated from the relative abundance (MNI%) of the identified mollusc remains by XU. Exposed (high energy) environments correlate to surf beaches, while sheltered (low energy) environments would be estuaries and sheltered bays. As all taxa can occupy sandy substrates, the comparison between sand and mud habitat is a probabilistic indication of mud-tolerant taxa increasing through time.

barrier, and also in sections along the lagoon-side as the estuary began to form (Figures 9–11).

The Stage 4 reconstructions are largely based on the excavated archaeological mollusc taxa's habitats. An estuarine environment formed sometime between 1,350 and 970 cal BP (Wk-56450, Wk-56701 at 95.4% probability). Sediment infill created extensive sandy intertidal and subtidal flats. People foraged for both *Latona deltoides* (pipis) and *Katelysia* spp. (sand cockles). The actively forming sheltered sandy tidal flats provided habitats for *Katelysia* spp., while *Latona deltoides* habitats simultaneously declined and largely disappears from the lagoon-side beach. *Latona deltoides* habitats were now restricted to the high-energy, ocean-facing surf beach.

In Stage 5, dated from 1,050 cal BP onwards (Wk-56453: 1,050–930 cal BP; Wk-56446: 800–680 cal BP; Wk-56700: 680–460 cal BP; Wk-56444: 660–550 cal BP; Wk-56445: 630–520 cal BP), the lagoon continued to infill with likely contributions from terrestrial sediments. The dune barrier to the open ocean expanded longitudinally, reducing the sea passage between the lagoon and the open ocean. This resulted in less tidal flux and in the increased siltation of the lagoon sandflats, creating areas of mudflat. The lagoon became more sheltered as the barrier further closed (Figure 11). These changes brought about conditions ideal for the growth of *Anapella cycladea*, which became an important contributor to the midden after 800 cal BP (McLoughlins Beach 1: Wk-56446; Figure 10). From c. 1,000 cal BP onwards, terrestrial

vegetation further developed on the dune barrier, particularly shrub and tree species. This is suggested by a major increase in charcoal fragments in SU2 of the McLoughlins Beach 1 sequence, dating from 800 cal BP (Wk-56446) to at least 520 cal BP (Wk-56444, Wk-56445). The presence of abundant wood charcoal and ash in the sediments, extending beyond the immediate area of the middens for hundreds of meters along the exposed dune-face, signals the presence of abundant woody plant taxa in the immediate vicinity of the site.

There is a stark difference in layer characteristics between SU2 at McLoughlins Beach 1 (dark gray sand, dense charcoal, *Katelysia* spp. and *A. cycladea* shell taxa) and SU3 (yellow sand, infrequent and sparse, dispersed charcoal, *Latona deltoides* and *Katelysia* spp. shell taxa). The dating of these two phases from 800 to 460 cal BP for SU2, and 1,820 to 970 cal BP for SU3, indicates that the change took place between 800 cal BP and 970 cal BP (Table 1). The differences in charcoal contents in the sediments of the two SUs are likely the product of abundant fuel in the immediate area for campfires in SU2, whereas previously in SU3 the vegetation on the dunes was probably less woody (e.g., grasses, sedges). Similarly, as the littoral habitats changed, people continued to gather shellfish, leaving behind an archaeological record of multiple shell species that reflected the changing habitats. Figure 10 indicates that the changes in relative abundance of *L. deltoides, Katelysia* spp. and *A. cycladea* took place rapidly especially between XU27 and XU26, representing the transition from SU3 to the SU3–SU2 interface
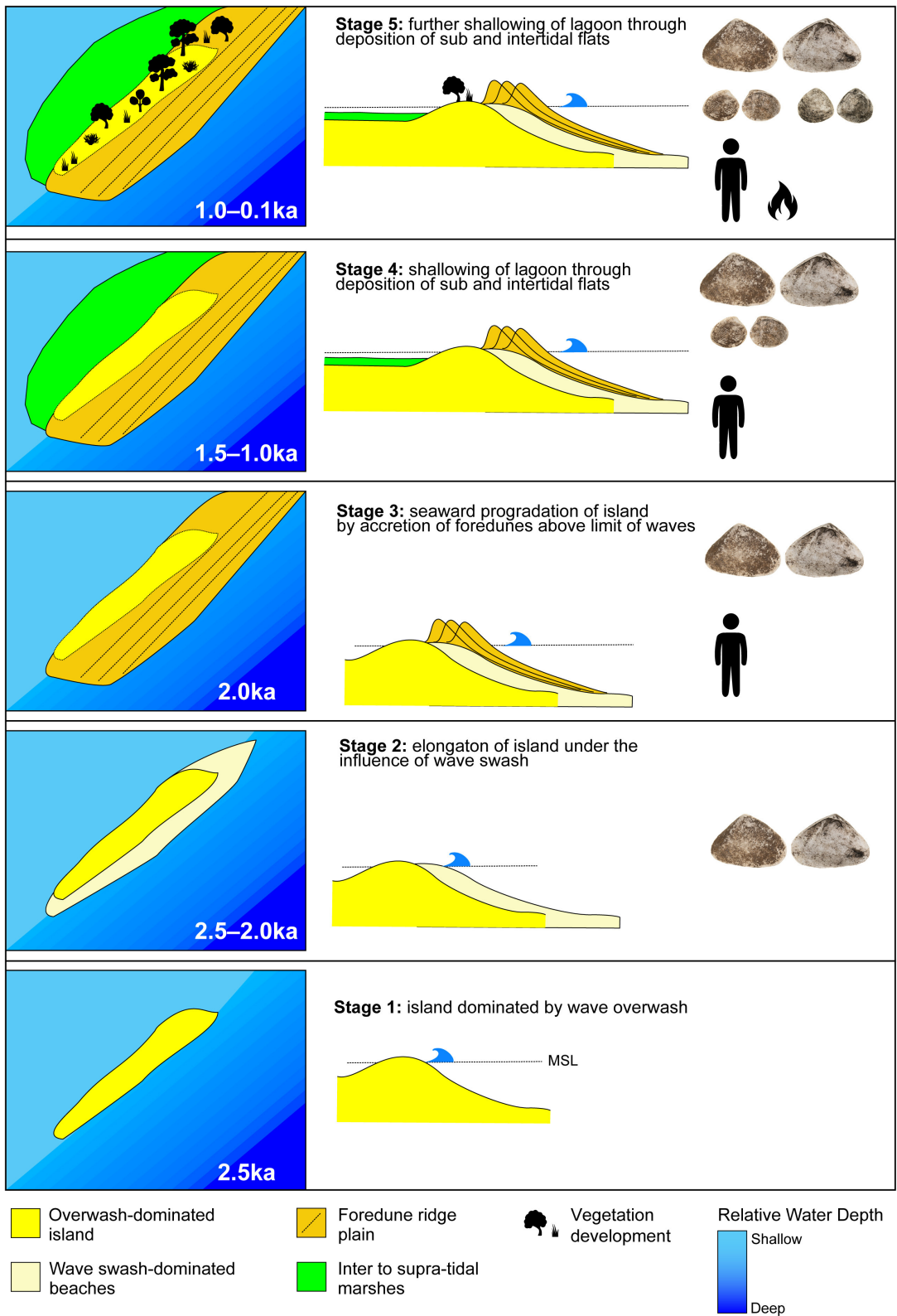
FIGURE 11
Evolutionary sequence for the McLoughlins Beach barrier dune system with associated date ranges, presence of people and gathered shellfish taxa, as indicated by the McLoughlins Beach 1 and 2 excavations.

and dating to sometime between 1,750 and 1,120 cal BP (Wk-56447, Wk-56701).

In early post-colonial times it appears that people stopped regularly camping in the area. This also corresponds to a period of landscape instability as indicated by fine sand overlying the archaeological site, with the young age of the overlying sand revealed by the post-1700s CE radiocarbon and OSL ages at McLoughlins Beach 1 (Wk-56443: 260–0 cal BP at the base of SU1C; OSL age of 0.13 ± 0.01 ka in the center of SU1C). This period of landscape instability is certainly regional in nature along Ninety-Mile Beach, with a widespread unconformity between stable land surfaces indicated by buried soil profiles being found along the shoreline for 100 km northwards (Kennedy et al., 2020). Such geomorphic changes are still occurring today, with the region's dunes in a process of revegetation in the past few decades (Gao et al., 2023) and landscape stability only recently returning to the region. It is also worth noting that the southern extent of the McLoughlins Barrier was larger in the past, as its current southern limit is defined by a channel (New Entrance) that was cut during storm overwash in 1961 (Rosengren, 2013).

It has been well documented both archaeologically/palaeo-biogeographically and anthropologically that Aboriginal peoples undertook systematic, landscape-scale burns of Country to manage the landscape (cultural burning) across much, and probably all, of Australia (e.g., Bliege Bird et al., 2008; Bliege Bird and Bird, 2021; Buettel et al., 2023; David et al., 2024; Fletcher et al., 2021; Jones, 2012). Anthropogenic landscape burning has been documented from over 40,000 years ago in Tasmania (Lutruwita; Adeleye et al., 2024). Cultural burning is a sophisticated cultural practice whereby low-level landscape-scale fires are used to manage patches of Country (land, plants, and animals) and improve the health of Country and its people. Cultural burning is low-temperature, low-flame burning of ground-level vegetation such as grasses, understorey vegetation and leaf litter, and does not burn "ladder fuels" that rise to the tree-tops (Buettel et al., 2023; David et al., 2024). The reduction of grasses, leaf litter and dense low-story vegetation through fire cleared the ground prior to camping, increased ground visibility (and the visibility of venomous snakes), enhanced biodiversity across the landscape, facilitated travel, and promoted nutritious vegetation growth that attracted grazing animals such as wallabies (David et al., 2024). It also announced the rightful presence of individuals and families through smoke and signs of ancestrally ordained landscape management practices through visible burnt patches and mosaics of land. The coasts and dunes were no exception to cultural burning practices. They were (and continue to be) favored camping places with rich "bush tucker" (plant and animal) foods and medicines that required landscape management (Buettel et al., 2023; David et al., 2024; Rowe et al., 2023). The ash-stained SU2 (c. 800 to 520 cal BP) horizon that extends continuously for more than 800 m along the exposed dune-face, including well beyond the extent of shell middens, suggests that much of the charcoal and ash may not relate to individual fireplaces, but rather to landscape-scale land management practices. As cultural burning in coastal zones is a low-temperature fire of mostly grasses and leaves (David et al., 2024), it is most often represented by extensive ashy sediments. This differs from campfires and fast-moving natural bushfires,

which are frequently evidenced by larger charcoal particles from burnt wood. The extensive ash staining of SU2 is more likely the product of coastal cultural burning, which would have shaped and maintained vegetation communities and their associated faunal populations, and accelerated sediment mobilization that contributed to the dynamics of landforms and river, lake and marine sedimentation. As such, landscape burning practices along the Nooramunga coast in SU2 over the past c. 750 years may have accelerated siltation of the lagoon, thus creating or accelerating environmental conditions for *A. cycladea* to thrive. It is impossible to determine at this stage if inshore habitat transformation in favor of *A. cycladea* and *Katelysia* spp. populations was also an end-goal. But this is certainly possible, and the influence of terrestrial cultural landscapes on promoting desirable marine biota has been noted elsewhere in the Pacific Islands (Rogers and Weisler, 2024).

Overall, archaeological and geomorphic investigations at the McLoughlins Beach excavations and associated beach barrier system demonstrate how rapidly people living along the southeastern Australian coast adapted to their changing environments. People utilized molluscan resources at the McLoughlins Beach barrier system as soon as the overwash process ceased, dune development occurred, and *Latona deltoides* became available. They repeatedly camped in the immediate area of the Nooramunga Midden Complex for over 1,000 years, as the surrounding landscape rapidly changed from a high-energy, open surf beach to partially protected sandflats, to sheltered mudflats, and effectively utilized the changing habitats and their respective shellfish species throughout these transformations. The GunaiKurnai Old Ancestors living along the coast co-created their landscapes through practices of landscape management through cultural burning, opening up the dune system's dense low-story vegetation cover to camping activities (Buettel et al., 2023; David et al., 2024; Fletcher et al., 2021) and simultaneously accelerating siltation of the lagoon in the process.

The dynamic nature of coastal landscapes, driven by climate change, sea-level fluctuations and attendant biotic adjustments, has had profound impacts on human communities in the past. So too have the particular cultural practices of cultural burning. Coastal environments and ecosystems have both challenged and sustained human populations, offering abundant resources while also requiring adaptability. Human populations have consistently demonstrated resilience in the face of changing coastal landscapes, whether through adaptive foraging and food production, re-settlement, expansion of social networks, and/or transforming the seascapes in return. These responses and initiatives provide valuable insights into the long-term interactions between people and their environments, offering lessons for understanding contemporary challenges to climate change and sea level rise.

Data availability statement

The original contributions presented in the study are included in the article/Supplementary material, further inquiries can be directed to the corresponding author.

Author contributions

AR: Conceptualization, Formal analysis, Investigation, Methodology, Project administration, Writing – original draft, Writing – review & editing. DK: Conceptualization, Formal analysis, Funding acquisition, Investigation, Methodology, Project administration, Writing – original draft, Writing – review & editing. BD: Conceptualization, Funding acquisition, Investigation, Methodology, Project administration, Resources, Writing – review & editing. RM: Funding acquisition, Resources, Supervision, Writing – review & editing. JF: Funding acquisition, Resources, Supervision, Writing – review & editing. FP: Formal analysis, Methodology, Resources, Writing – review & editing. LA: Formal analysis, Methodology, Resources, Writing – review & editing. MD: Formal analysis, Methodology, Resources, Writing – review & editing. GLaWAC: Funding acquisition, Resources, Supervision, Writing – review & editing. CD: Investigation, Writing – review & editing. HM: Investigation, Writing – review & editing.

Funding

Acknowledgments

Conflict of interest

The authors declare that the research was conducted in the absence of any commercial or financial relationships that could be construed as a potential conflict of interest.

Generative AI statement

The author(s) declare that no Gen AI was used in the creation of this manuscript.

Publisher's note

All claims expressed in this article are solely those of the authors and do not necessarily represent those of their affiliated organizations, or those of the publisher, the editors and the reviewers. Any product that may be evaluated in this article, or claim that may be made by its manufacturer, is not guaranteed or endorsed by the publisher.

Supplementary material

The Supplementary Material for this article can be found online at: https://www.frontiersin.org/articles/10.3389/fearc.2025.1548062/full#supplementary-material

References

Adeleye, M., Hopf, F., Haberle, S. G., Stannard, G. L., McWethy, D. B., Harris, S., et al. (2024). Landscape burning facilitated Aboriginal migration into Lutruwita/Tasmania 41,600 years ago. *Sci. Adv.* 10:eadp6579. doi: 10.1126/sciadv.adp6579

Arnold, L. J., Demuro, M., Power, R., Priya, Duval, M., Guilarte, V., Weij, R., et al. (2022). Examining sediment infill dynamics at Naracoorte Cave megafauna sites using multiple luminescence dating signals. *Quat. Geochronol.* 70:101301. doi: 10.1016/j.quageo.2022.101301

Arnold, L. J., Demuro, M., Spooner, N. A., Prideaux, G. J., McDowell, M. C., Camens, A. B., et al. (2019). Single-grain TT-OSL bleaching characteristics: insights from modern analogues and OSL dating comparisons. *Quat. Geochronol.* 49, 45–51. doi: 10.1016/j.quageo.2018.01.004

Arnold, L. J., Duval, M., Demuro, M., Spooner, N. A., Santonja, M., and Pérez-González, A. (2016). OSL dating of individual quartz 'supergrains' from the Ancient Middle Palaeolithic site of Cuesta de la Bajada, Spain. *Quat. Geochronol.* 36, 78–101. doi: 10.1016/j.quageo.2016.07.003

Arnold, L. J., and Roberts, R. G. (2009). Stochastic modelling of multi-grain equivalent dose (De) distributions: implications for OSL dating of sediment mixtures. *Quat. Geochronol.* 4, 204–230. doi: 10.1016/j.quageo.2008.12.001

Arnold, L. J., Roberts, R. G., Galbraith, R. F., and DeLong, S. B. (2009). A revised burial dose estimation procedure for optical dating of young and modern-age sediments. *Quat. Geochronol.* 4, 306–325. doi: 10.1016/j.quageo.2009.02.017

Arnold, L. J., Roberts, R. G., Macphee, R. D. E., Willerslev, E., Tikhonov, A. N., and Brock, F. (2008). Optical dating of perennially frozen deposits associated with preserved ancient plant and animal DNA in north-central Siberia. *Quat. Geochronol.* 3, 114–136. doi: 10.1016/j.quageo.2007.09.002

Bailey, R. M., and Arnold, L. J. (2006). Statistical modelling of single grain quartz De distributions and an assessment of procedures for estimating burial dose. *Quat. Sci. Rev.* 25, 2475–2502. doi: 10.1016/j.quascirev.2005.09.012

Barker, B. C. (1991). Nara Inlet 1: Coastal resource use and the Holocene marine transgression in the Whitsunday Islands, central Queensland. *Archaeol. Ocean.* 26, 102–109. doi: 10.1002/j.1834-4453.1991.tb00273.x

Barnett, R. L., Charman, D. J., Johns, C., Ward, S. L., Bevan, A., Bradley, S. L., et al. (2020). Nonlinear landscape and cultural response to sea-level rise. *Sci. Adv.* 6:eabb6376. doi: 10.1126/sciadv.abb6376

Bliege Bird, R., and Bird, D. W. (2021). Climate, landscape diversity, and food sovereignty in arid Australia: the firestick farming hypothesis. *Am. J. Hum. Biol.* 33:e23527. doi: 10.1002/ajhb.23527

Bliege Bird, R., Bird, D. W., Codding, B. F., Parker, C. H., and Jones, J. H. (2008). The "fire stick farming" hypothesis: Australian Aboriginal foraging strategies, biodiversity, and anthropogenic fire mosaics. *Proc. Natl. Acad. Sci. U.S.A.* 105, 14796–14801. doi: 10.1073/pnas.0804757105

Bowdler, S. (1976). Hook, line and dilly bag: an interpretation of an Australian coastal shell midden. *Mankind* 10, 248–258. doi: 10.1111/j.1835-9310.1999.tb01453.x

Bowler, J. M., Johnston, H., Olley, J. M., Prescott, J. R., Roberts, R. G., Shawcross, W., et al. (2003). New ages for human occupation and climatic change at Lake Mungo, Australia. *Nature* 421, 837–840. doi: 10.1038/nature01383

Boyd, S. (2011). *Taxonomic Toolkit for Marine Life of Port Phillip Bay, Port Phillip Marine Life*. Available online at: https://portphillipmarinelife.net.au/ (accessed June 6, 2023).

Brennan, B. J. (2003). Beta doses to spherical grains. *Radiat. Measure.* 37, 299–303. doi: 10.1016/S1350-4487(03)00011-8

Brisset, E., Burjachs, F., Ballesteros Navarro, B. J., and Fernández-López de Pablo, J. (2018). Socio-ecological adaptation to Early-Holocene sea-level rise in the western Mediterranean. *Glob. Planet. Change.* 169, 156–167. doi: 10.1016/j.gloplacha.2018.07.016

Bronk Ramsey, C. (2009). Bayesian analysis of radiocarbon dates. *Radiocarbon* 51, 337–360. doi: 10.1017/S0033822200033865

Buettel, J., David, B., Mullett, R., Fresløv, J., Szabó, K., and GunaiKurnai Land and Waters Aboriginal Corporation (eds.). (2023). *Fires in GunaiKurnai Country Landscape Fires and their Impacts on Aboriginal Cultural Heritage Places and Artefacts in Southeastern Australia*. Oxford: Archaeopress Archaeology. doi: 10.2307/jj.15136002

Carson, M. T., and Athens, J. S. (2007). Integration of coastal geomorphology, mythology, and archaeological evidence at Kualoa Beach, windward O'ahu, Hawaiian Islands. *J. Island Coastal Archaeol.* 2, 24–43. doi: 10.1080/15564890701219693

Chen, Z., Wang, Z., Schneiderman, J., Tao, J., and Cai, Y. (2005). Holocene climate fluctuations in the Yangtze delta of eastern China and the Neolithic response. *Holocene* 15, 915–924. doi: 10.1191/0959683605hl862rr

Cobb, K., Charles, C., Cheng, H., and Edwards, L. (2003). El Nino/Southern oscillation and tropical Pacific climate during the last millennium *Nature* 424, 271–276. doi: 10.1038/nature01779

Codding, B. F., O'Connell, J. F., and Bird, D. W. (2014). Shellfishing and the colonization of Sahul: a multivariate model evaluating the dynamic effects of prey utility, transport considerations and life-history on foraging patterns and midden composition. *J. Island Coastal Archaeol.* 9, 238–252. doi: 10.1080/15564894.2013.848958

Collerson, K. D., and Weisler, M. I. (2007). Stone adze compositions and the extent of ancient Polynesian voyaging and trade. *Science* 317, 1907–1911. doi: 10.1126/science.1147013

David, B., Aplin, K., Peck, H., Skelly, R., Leavesley, M., Mialanes, J., et al. (2020). "Moiapu 3: settlement on Moiapu Hill at the very end of Lapita, Caution Bay hinterland," in *Debating Lapita: Distribution, Chronology, Society and Subsistence*, eds. S. Bedford and M. Spriggs (Canberra, ACT: ANU Press), 61–88. doi: 10.22459/TA52.2019.03

David, B., Fletcher, M. S., Connor, S., Pullin, V. R., Birkett-Rees, J., Delannoy, J. J., et al. (2024). *Cultural Burning. Elements in Current Archaeological Tools and Techniques*. Cambridge: Cambridge University Press. doi: 10.1017/9781009485340

Demuro, M., Arnold, L. J., González-Urquijo, J., Lazuen, T., and Frochoso, M. (2023). Chronological constraint of Neanderthal cultural and environmental changes in southwestern Europe. MIS 5–MIS 3 dating of the Axlor site (Biscay, Spain). *J. Quat. Sci.* 38, 890–920. doi: 10.1002/jqs.3527

Erlandson, J. M., and Braje, T. J. (2015). Coasting out of Africa: the potential of mangrove forests and marine habitats to facilitate human coastal expansion via the Southern Dispersal Route. *Quat. Int.* 382, 31–41. doi: 10.1016/j.quaint.2015.03.046

Erlandson, J. M., Braje, T. J., Gill, K. M., and Graham, M. H. (2015). Ecology of the kelp highway: did marine resources facilitate human dispersal from northeast Asia to the Americas? *J. Island Coastal Archaeol.* 10, 1–20. doi: 10.1080/15564894.2014.1001923

Faulkner, P., Sarathi, A., Crowther, A., Smith, T., Harris, M., Ali, A. K., et al. (2022). Human-ecodynamics and the intertidal zones of the Zanzibar Archipelago. *Front. Earth Sci.* 10:982694. doi: 10.3389/feart.2022.982694

Field, J. S., and Lape, P. V. (2010). Paleoclimates and the emergence of fortifications in the tropical Pacific islands. *J. Anthropol. Archaeol.* 29, 113–124. doi: 10.1016/j.jaa.2009.11.001

Fitzpatrick, S. M. (2009). "Exploration and discovery," in *Encyclopedia of Islands*, eds. R. Gillespie and D. Clague (Berkeley, CA: University of California Press), 276–281. doi: 10.1525/9780520943728-066

Fitzpatrick, S. M., and Anderson, A. (2008). Islands of isolation: archaeology and the power of aquatic perimeters. *J. Island Coastal Archaeol.* 3, 4–16. doi: 10.1080/15564890801983941

Fitzpatrick, S. M., and Giovas, C. M. (2021). Tropical islands of the Anthropocene: deep histories of anthropogenic terrestrial-marine entanglement in the Pacific and Caribbean. *Proc. Natl. Acad. Sci. U.S.A.* 118:e2022209118. doi: 10.1073/pnas.2022209118

Fletcher, M. S., Romano, A., Connor, S., Mariani, M., and Maezumi, S. Y. (2021). Catastrophic bushfires, Indigenous fire knowledge and reframing science in southeast Australia. *Fire* 4:61. doi: 10.3390/fire4030061

Galbraith, R. F., Roberts, R. G., Laslett, G. M., Yoshida, H., and Olley, J. M. (1999). Optical dating of single and multiple grains of quartz from Jinmium rock shelter,

northern Australia: part I, experimental design and statistical models. *Archaeometry* 41, 339–364. doi: 10.1111/j.1475-4754.1999.tb00987.x

Gao, J., Kennedy, D. M., and McSweeney, S. (2023). Patterns of vegetation expansion during dune stabilization at the decadal scale. *Earth Surf. Process. Landf.* 48, 3059–3073. doi: 10.1002/esp.5681

Guérin, G., Mercier, M., and Adamiec, G. (2011). Dose-rate conversion factors: update. *Ancient TL* 29, 5–8. doi: 10.26034/la.atl.2011.443

GunaiKurnai Land and Waters Aboriginal Corporation (2015). *GunaiKurnai Whole-of-Country Plan. GunaiKurnai Land and Waters Aboriginal Corporation, Bairnsdale, Victoria, Australia*. Available online at: https://gunaikurnai.org/wp-content/uploads/2021/07/Gunaikurnai-Whole-of-Country-Plan-ONLINE.pdf (accessed June 18, 2023).

Gusick, A. E., Maloney, J., Braje, T. J., Retallack, G. J., Johnson, L., Klotsko, S., et al. (2022). Soils and terrestrial sediments on the seafloor: Refining archaeological paleoshoreline estimates and paleoenvironmental reconstruction off the California coast. *Front. Earth Sci.* 10:941911. doi: 10.3389/feart.2022.941911

Harris, M., Weisler, M., and Faulkner, P. (2015). A refined protocol for calculating MNI in archaeological molluscan shell assemblages: a Marshall Islands case study. *J. Archaeol. Sci.* 57, 168–179. doi: 10.1016/j.jas.2015.01.017

Heaton, T. J., Köhler, P., Butzin, M., Bard, E., Reime, R. W., Austin, W. E. N., et al. (2020). Marine20—the marine radiocarbon age calibration curve (0–55,000 cal BP). *Radiocarbon* 62, 1–42. doi: 10.1017/RDC.2020.68

Heldt, K., and Hart, A. (2021). *Vongoles 2020*. Fisheries Research and Development Corporation. Available online at: https://www.fish.gov.au/report/269-VONGOLES-2020 (accessed November 6, 2023).

Heldt, K., and Mayfield, S. (2020). *Harvestable biomass of Katelysia spp. in the South Australian Vongole Fishery*. Unpublished report prepared for PIRSA Fisheries and Aquaculture. South Australian Research and Development Institute (Aquatic Sciences), Adelaide, South Australia, Australia. SARDI Publication Number. F2014/000191-2. SARDI Research Report Series No. 1060.

Hibbert, F. D., Williams, F. H., Fallon, S. J., and Rohling, E. J. (2018). A database of biological and geomorphological sea-level markers from the Last Glacial Maximum to present. *Sci. Data* 5:180088. doi: 10.1038/sdata.2018.88

Hogg, A., Heaton, T. J., Hua, Q., Palmer, J., Turney, C., Southon, J., et al. (2020). SHCAL20 Southern Hemisphere calibration, 0-55,000 years cal BP. *Radiocarbon* 62, 759–778. doi: 10.1017/RDC.2020.59

Hristova, R., and Peev, P. (2014). Sea level rise and human adaptation to environmental changes during the late prehistory along the Western Black Sea coast. *Comptes rendus de l'Académie bulgare Sci.* 67, 693–699.

Hughes, M. G., and Heap, A. D. (2010). National-scale wave energy resource assessment for Australia. *Renew. Energy* 35, 1783–1791. doi: 10.1016/j.renene.2009.11.001

Ierodiaconou, D., Kennedy, D. M., Pucino, N., Allan, B. M., McCarroll, R. J., Ferns, L. W., et al. (2022). Citizen science unoccupied aerial vehicles: a technique for advancing coastal data acquisition for management and research. *Continent. Shelf Res.* 244:104800. doi: 10.1016/j.csr.2022.104800

Jacobs, Z., Duller, G. A. T., Wintle, A. G., and Henshilwood, C. S. (2006). Extending the chronology of deposits at Blombos Cave, South Africa, back to 140 ka using optical dating of single and multiple grains of quartz. *J. Hum. Evol.* 51, 255–273. doi: 10.1016/j.jhevol.2006.03.007

Jacobs, Z., Jankowski, N. R., Dibble, H. L., Goldberg, P., McPherron, S. J., Sandgathe, D., et al. (2016). The age of three Middle Palaeolithic sites: single-grain optically stimulated luminescence chronologies for Pech de l'Azé I, II and IV in France. *J. Hum. Evol.* 95, 80–103. doi: 10.1016/j.jhevol.2016.03.010

Johns, D. A., Irwin, G., and Sung, Y. K. (2014). An early sophisticated East Polynesian voyaging canoe discovered on New Zealand's coast. *Proc. Natl. Acad. Sci. U.S.A.* 111, 14728–14733. doi: 10.1073/pnas.1408491111

Jones, R. (2012). Fire-stick farming. *Fire Ecol.* 8, 3–8. doi: 10.1007/BF03400623

Kennedy, D. M., Oliver, T. S. N., Tamura, T., Murray-Wallace, C. V., Thom, B. G., Rosengren, N. J., et al. (2020). Holocene evolution of the Ninety Mile Beach sand barrier, Victoria, Australia: the role of sea level, sediment supply and climate. *Marine Geol.* 430:106366. doi: 10.1016/j.margeo.2020.106366

Kennedy, D. M., Thom, B., Gell, R., and Rosengren, N. J. (2024). Coastal geomorphology and geology of the Gippsland Lakes region: a review and future directions. *Proc. R. Soc. Vict.* 136. doi: 10.1071/RS23018

Krapivner, R. B. (2020). The last global transgression of the world ocean: Glacio-eustasy or tectonics? *Geotectonics* 54, 477–493. doi: 10.1134/S0016852120040056

Lamb, L., and Barker, B. (2001). Evidence for Early Holocene change in the Whitsunday Islands: a new radiocarbon determination from Nara Inlet 1. *Aust. Archaeol.* 53, 42–43. doi: 10.1080/03122417.2001.11681722

Lewis, R. J., Tibby, J., Arnold, L. J., Barr, C., Marshall, J., McGregor, G., et al. (2020). Insights into subtropical Australian aridity from Welsby Lagoon, north Stradbroke Island, over the past 80,000 years. *Quat. Sci. Rev.* 234:106262. doi: 10.1016/j.quascirev.2020.106262

Marwick, B., Van Vlack, H. G., Conrad, C., Shoocongdej, R., Thongcharoenchaikit, C., and Kwak, S. (2017). Adaptations to sea level change and transitions to agriculture at Khao Toh Chong rockshelter, Peninsular Thailand. *J. Archaeol. Sci.* 77, 94–108. doi: 10.1016/j.jas.2016.10.010

McCoy, M. D., Alderson, H. A., Hemi, R., Cheng, H., and Edwards, R. L. (2016). Earliest direct evidence of monument building at the archaeological site of Nan Madol (Pohnpei, Micronesia) identified using 230Th/U coral dating and geochemical sourcing of megalithic architectural stone. *Quat. Res.* 86, 295–303. doi: 10.1016/j.yqres.2016.08.002

Meehan, B. (1982). *Shell Bed to Shell Midden.* Canberra, ACT: Australian Institute of Aboriginal Studies.

Mejdahl, V. (1979). Thermoluminescence dating: beta-dose attenuation in quartz grains. *Archaeometry* 21, 61–72 doi: 10.1111/j.1475-4754.1979.tb00241.x

Mejdahl, V. (1987). Internal radioactivity in quartz and feldspar grains. *Ancient TL* 5, 10–17. doi: 10.26034/la.atl.1987.119

Moss, M. L. (2013). "Fishing traps and weirs on the Northwest coast of North America: new approaches and new insights," in *The Oxford Handbook of Wetland Archaeology*, eds. F. Menotti and A. Sullivan (Oxford: Oxford University Press), 323–337. doi: 10.1093/oxfordhb/9780199573493.013.0020

Nakajima, T., Hudson, M. J., Uchiyama, J., Makibayashi, K., and Zhang, J. (2019). Common carp aquaculture in Neolithic China dates back 8,000 years. *Nat. Ecol. Evol.* 3, 1415–1418. doi: 10.1038/s41559-019-0974-3

Nunn, P. D., Hunter-Anderson, R., Carson, M. T., Thomas, F., Ulm, S., and Rowland, M. J. (2007). Times of plenty, times of less: last-millennium societal disruption in the Pacific Basin. *Hum. Ecol.* 35, 385–401. doi: 10.1007/s10745-006-9090-5

O'Grady, J. G., McInnes, K. L., Colberg, F., Hemer, M., and Badanin, A. V. (2015). Longshore wind, waves and currents: climate and climate projections at Ninety Mile Beach, southeastern Australia. *Int. J. Climatol.* 35, 4079–4093. doi: 10.1002/joc.4268

Pawley, S. M., Bailey, R. M., Rose, J., Moorlock, B. S. P., Hamblin, R. J. O., Booth, S. J., et al. (2008). Age limits on Middle Pleistocene glacial sediments from OSL dating, north Norfolk, UK. *Quat. Sci. Rev.* 27, 1363–1377. doi: 10.1016/j.quascirev.2008.02.013

Pawlik, A. F., Piper, P. J., Faylona, M. G. P. G., Padilla, S. G., Carlos, J., Mijares, A. S., et al. (2014). Adaptation and foraging from the terminal Pleistocene to the Early Holocene: excavation at Bubog on Ilin island, Philippines. *J. Field Archaeol.* 39, 230–247. doi: 10.1179/0093469014Z.00000000090

Pedergnana, A., Cristiani, E., Munro, N., Valletta, F., and Sharon, G. (2021). Early line and hook fishing at the Epipaleolithic site of Jordan River Dureijat (Northern Israel). *PLoS ONE* 16:e0257710. doi: 10.1371/journal.pone.0257710

Prescott, J. R., and Hutton, J. T. (1994). Cosmic ray contributions to dose rates for luminescence and ESR dating: large depths and long-term time variations. *Radiat. Measure.* 23, 497–500. doi: 10.1016/1350-4487(94)90086-8

Propeller. (2023). *How Accurate are AeroPoints?* Available online at: https://www.propelleraero.com/blog/propeller-ppk-how-many-aeropoints-does-it-take-to-get-accurate-results/ (accessed November 10, 2024).

Pucino, N., Kennedy, D. M., Carvalho, R. C., Allan, B., and Ierodiaconou, D. (2021). Citizen science for monitoring seasonal-scale beach erosion and behaviour with aerial drones. *Sci. Rep.* 11:3935. doi: 10.1038/s41598-021-83477-6

Rees-Jones, J. (1995). Optical dating of young sediments using fine-grain quartz. *Ancient TL* 13, 9–14. doi: 10.26034/la.atl.1995.242

Rees-Jones, J., and Tite, M. S. (1997). Optical dating results for British archaeological sediments. *Archaeometry* 39, 177–187. doi: 10.1111/j.1475-4754.1997.tb00797.x

Reitz, E. J., and Wing, E. S. (2008). *Zooarchaeology.* Cambridge: Cambridge University Press. doi: 10.1017/CBO9780511841354

Rogers, A. J. (2023). Aquaculture in the ancient world: ecosystem engineering, domesticated landscapes, and the first Blue Revolution. *J. Archaeol. Res.* 32, 427–491 doi: 10.1007/s10814-023-09191-1

Rogers, A. J., and Weisler, M. I. (2022). Risk, reliability, and the importance of small-bodied molluscs across the Hawaiian windward-leeward divide. *Hum. Ecol.* 50, 141–165. doi: 10.1007/s10745-021-00297-y

Rogers, A. J., and Weisler, M. I. (2024). Terrestrial cultural landscapes changed inshore marine ecosystems: eight centuries of shellfish harvesting from the Kawela Mound site, Hawaiian Islands. *Holocene.* 34, 487–503. doi: 10.1177/09596836231219474

Rosengren, N. (2013). Ninety *Mile Beach Barriers and Dunes.* Melbourne, VIC: Water Technology P/L.

Rowe, C., David, B., Mialanes, J., Ulm, S., Petchey, F., Aird, S., et al. (2020). A Holocene record of savanna vegetation dynamics in southern lowland Papua New Guinea. *Veg. Hist. Archaeobot.* 29, 1–14. doi: 10.1007/s00334-019-00724-7

Rowe, C., Stevenson, J., Connor, S., and Adeleye, M. (2023). "Fire and the transformation of landscapes," in *The Oxford Handbook of the Archaeology of Indigenous Australia and New Guinea*, eds. I. J. McNiven and B. David (Oxford: Oxford University Press), 381–411. doi: 10.1093/oxfordhb/9780190095611.013.12

Rowland, M. J., and Ulm, S. (2011). Indigenous fish traps and weirs of Queensland. *Queensl. Archaeol. Res.* 14, 1–58. doi: 10.25120/qar.14.2011.219

Salomon, A. K., and McKechnie, I. (2025). Insights gained from including people in our models of nature and modes of science. *Annu. Rev. Marine Sci.* 17, 23.1–23.25. doi: 10.1146/annurev-marine-021523-105524

Schmich, S. A. (2013). *The archaeology of Local Human response to an environmental transformation* (PhD dissertation). Arizona State University, Tempe, Arizona.

Skelly, R. J., and David, B. (2017). *Hiri: Archaeology of Long-distance Maritime Trade along the South Coast of Papua New Guinea.* Honolulu: University of Hawai'i Press.

Smith, N. F., Lepofsky, D., Toniello, G., Holmes, K., Wilson, L., Neudorf, C. M., et al. (2019). 3500 years of shellfish mariculture on the Northwest Coast of North America. *PLoS ONE* 14:e0211194. doi: 10.1371/journal.pone.0211194

Surdez, M., Beck, J., Sakellariou, D., Vogel, H., Emery, P. B., Koutsoumba, D., et al. (2018). Flooding a landscape: impact of Holocene transgression on coastal sedimentology and underwater archaeology in Kiladha Bay (Greece). *Swiss J. Geosci.* 111, 573–588. doi: 10.1007/s00015-018-0309-4

Thompson, V. D., Marquardt, W. H., and Walker, K. J. (2014). A remote sensing perspective on shoreline modification, canal construction and household trajectories at Pineland along Florida's southwestern Gulf Coast. *Archaeol. Prospect.* 21, 59–73. doi: 10.1002/arp.1470

Thompson, V. D., Marquardt, W. H., Walker, K. J., Roberts Thompson, A., and Newsom, L. A. (2018). Collective action, state building, and the rise of the Calusa, southwest Florida. *J. Anthropol. Archaeol.* 51, 28–44. doi: 10.1016/j.jaa.2018.05.003

Tribe, H. M., and Kennedy, D. M. (2010). The geomorphology and evolution of a large barrier spit: Farewell Spit, New Zealand. *Earth Surf. Process. Landf.* 35, 1751–1762. doi: 10.1002/esp.2009

Ulm, S., O'Grady, D., Petchey, F., Hua, Q., Jacobsen, G., Linnenlucke, L., et al. (2023). Australian marine radiocarbon reservoir effects: ΔR atlas and ΔR calculator for Australian mainland coasts and near-shore islands. *Radiocarbon* 65, 1139–1159. doi: 10.1017/RDC.2023.95

Will, M., Bader, G. D., Sommer, C., Cooper, A., and Green, A. (2022). Coastal adaptations on the eastern seaboard of South Africa during the Pleistocene and Holocene? Current evidence and future perspectives from archaeology and marine geology. *Front. Earth Sci.* 10:964423. doi: 10.3389/feart.2022.964423

WoRMS Editorial Board (2024). *World Register of Marine Species.* Available online at: https://www.marinespecies.org (accessed October 18, 2024).

Zhuang, Y., and Kidder, T. R. (2014). Archaeology of the Anthropocene in the Yellow River region, China, 8000–2000 cal. BP. *Holocene* 24, 1602–1623. doi: 10.1177/0959683614544058